

national accelerator laboratory

pub
NAL-THY-54

June 1972

INELASTIC e^+e^- ANNIHILATION IN PERTURBATION THEORY

PAUL M. FISHBANE*

Physics Department, University of Virginia
Charlottesville, Virginia 22901

and

J. D. SULLIVAN**

National Accelerator Laboratory, Batavia, Illinois 60510

*Supported in part by the Center for Advanced Studies, University of Virginia.

**Permanent address: Physics Department, University of Illinois, Urbana, Illinois 61801.



Abstract

The structure functions for the annihilation process $e^+ + e^- \rightarrow \bar{P} + X$ are calculated in the neutral vector gluon model in the Bjorken limit. Bjorken scaling is broken by the presence of $\ln q^2$ factors in a way which is closely related to the situation in inelastic scattering. All calculations are carried out in a leading-logarithm approximation. In particular there is a multiplicity $n \sim \ln^2 q^2$ and a close interplay between the damping of the elastic form factor and the excitation of inelastic channels. The annihilation structure functions are shown to be related to their inelastic scattering counterparts by analytic continuation and by a physical region reciprocal relation. The reciprocal relation is observed to have a number of interesting consequences if it applies, in some approximate sense, to pion, protons, etc. In addition to the leading logarithm calculations contained in this paper the discussions given here of discontinuities of the virtual-Compton amplitude and the longitudinal impact parameter representation are of general interest and applicability.

1. INTRODUCTION

This paper is one in a series of papers¹⁻³ in which we study the neutral vector gluon model (massive QED) in the Bjorken scaling⁴ limit. The major topic of this paper is the annihilation channel⁵⁻⁷ $e^- + e^+ \rightarrow \bar{P} + X$, and the relation of the annihilation structure functions to their counterparts⁸ in inelastic scattering, $e^- + P \rightarrow e^- + X$. These relations may transcend the particular field theory studied here.

Here, as in all renormalizable^{9,10} (in contrast to superrenormalizable¹¹) field theories, strict Bjorken scaling is broken by the presence of $\ln q^2$ factors in the asymptotic expansion of the structure functions. We exploit this by calculating in a leading-logarithm approximation for a given order in perturbation theory and then summing the result to all orders in the coupling constant.

As for the inelastic scattering channel, the results we find for annihilation in the neutral vector gluon model differ greatly from the neutral pseudoscalar (scalar) field theory⁵ because of diagrams in which vector gluons are emitted and absorbed by the charged fermion line between the points at which the external current acts¹². These diagrams sum to an "infrared" type result and generate a multiplicity of (soft) vector mesons $\langle n \rangle \sim \ln^2 q^2$.

We find that, after appropriate interpretation, the annihilation structure functions can be reached by analytic continuation of the inelastic scattering structure functions. Furthermore we find and study a reciprocal relation, first explicitly noted by Gribov and Lipatov^{8,13}, which directly relates the annihilation and inelastic structure functions

in their respective physical regions.

In addition to our calculations for the neutral vector gluon model, occasional comparison to the pseudoscalar case and discussion of the reciprocal relation, our work here contains two formal sections which are of general interest and are not restricted to studies in perturbation theory. The first of these is in Sec. II where, after reviewing the kinematics, we state the various discontinuities of the virtual Compton amplitude which correspond to physical observables and the appropriate way to analytically continue from one to another¹⁴. While very little of this is truly new we feel it is useful to pull it together and emphasize the key points.

The other formal section is Sec. V, where we study the longitudinal impact parameter representation introduced in Ref. (5). After making the connection with Regge theory we go on to show how the longitudinal impact parameter representation provides a compact and efficient way to study the relations between the annihilation and inelastic structure functions.

The remaining sections of the work are as follows: In Sec. III, after briefly reviewing the leading-logarithm approximation which we use, we give the results for the annihilation structure functions in the neutral vector gluon model. Computational details are reserved for Appendix A. We also give the key properties: multiplicities, momentum distributions, etc., of the important final states which build up the annihilation cross section. In Sec. IV we discuss analytic continuation and the reciprocal relation between annihilation and scattering, using

the results of Sec. III. We also point out a convenient Lorentz frame in which these questions can be studied for arbitrary diagrams in any theory without explicit evaluation of all momentum integrations. We illustrate this with simple "diffractive" diagrams in γ_5 theory. Computational details are in Appendix B. In Sec. VI we discuss some of the physical consequences which would follow if the reciprocal relation were satisfied (in some approximate sense) by protons, pions, etc. This speculation is very tentative as we discuss in the same section. Finally in Sec. VII we give a very short summary of our results. Results for a cutoff theory are reserved for a future publication.

11. Summary of Kinematics and Structure Functions

In this work we are concerned with calculations of the annihilation process as well as the relation between annihilation and inelastic scattering. Consequently we begin with a brief review of kinematics and the structure functions for the two processes. To make clear the conditions imposed by crossing (substitution law) and analytic continuation it is also useful to identify the structure functions with certain discontinuities of the virtual Compton amplitude¹⁴.

It turns out to be helpful to consider simultaneously three distinct physical processes. They are:

Inelastic scattering

$$e^-(\ell) + H(p) \rightarrow e^-(\ell') + X, \quad (2.1a)$$

Three body annihilation

$$e^-(k^-) + e^+(k^+) + H(p) \rightarrow X, \quad (2.1b)$$

and

Annihilation

$$e^-(\ell^-) + e^+(\ell^+) \rightarrow \bar{H}(P) + X \quad (2.1c)$$

where X stands for the complete sum over the undetected hadron final states. The one-photon exchange approximations to these processes are shown in Fig. 1.

In each of the three cases we pick variables as follows:

Inelastic scattering

$$q^2 = (\ell - \ell')^2 < 0 \quad (2.2a)$$

$$v = p \cdot (\ell - \ell') / m > 0 \quad (2.3a)$$

$$\cos \theta_a = \hat{\ell}' \cdot \hat{\ell} \quad (2.4a)$$

Three body annihilation

$$q^2 = (k^- + k^+)^2 / m > 0 \quad (2.2b)$$

$$v = p \cdot (k^- + k^+) / m > 0 \quad (2.3b)$$

$$\cos \theta_b = \hat{k}^- \cdot \hat{k}^+ \quad (2.4b)$$

and,

Annihilation

$$q^2 = (\ell^- + \ell^+)^2 > 0 \quad (2.2c)$$

$$v = -P \cdot (\ell^- + \ell^+) / m < 0 \quad (2.3c)$$

$$\cos \theta_c = \hat{\ell} \cdot \hat{P}$$

Both $\cos \theta_a$ and $\cos \theta_b$ are measured in the hadron rest frame ($\underline{p}=0$), while $\cos \theta_c$ is measured in the center-of-mass frame ($\underline{q}=0$). [Note that according to Eq. (2.3c) v is the negative of the virtual photon energy in the frame $\underline{P}=0$.] For definiteness we will choose the hadron H to be a proton; m denotes its mass. All our remarks and equations will hold for any other choice for H provided m is always interpreted as the mass of H .

The physical regions for the three processes discussed above are shown together on Fig. 2. Note that had we not neglected the electron mass the processes 2.1(a) and 2.1(b) would be separated by a gap $\Delta q^2 = 4m_e^2$.

Aside from known factors associated with the electron lines and the virtual photon propagator, the spin averaged cross sections for the above processes are proportional to¹⁵

8.

$$\begin{aligned}
 \frac{1}{\pi} W^{\mu\nu}(\nu, q^2) &= \sum_n \langle P | j^\mu(0) | n \rangle \langle n | j^\nu(0) | P \rangle (2\pi)^3 \delta^4(p + q - p_n) \\
 &= \frac{1}{m^2} W_2(\nu, q^2) \left(p^\mu - \frac{p \cdot q}{q^2} q^\mu \right) \left(p^\nu - \frac{p \cdot q}{q^2} q^\nu \right) \\
 &\quad + W_1(\nu, q^2) \left(-g^{\mu\nu} + \frac{q^\mu q^\nu}{q^2} \right), \tag{2.5a}
 \end{aligned}$$

$$\begin{aligned}
 \frac{1}{\pi} \tilde{W}^{\mu\nu} &= \sum_n \langle P | j^\mu(0) | n \rangle_c \langle n | j^\nu(0) | P \rangle_c (2\pi)^3 \delta^4(p + q - p_n) \\
 &= \frac{1}{m^2} \tilde{W}_2(\nu, q^2) \left(p^\mu - \frac{p \cdot q}{q^2} q^\mu \right) \left(p^\nu - \frac{p \cdot q}{q^2} q^\nu \right) \\
 &\quad + \tilde{W}_1(\nu, q^2) \left(-g^{\mu\nu} + \frac{q^\mu q^\nu}{q^2} \right), \tag{2.5b}
 \end{aligned}$$

and

$$\begin{aligned}
 \frac{1}{\pi} \bar{W}^{\mu\nu}(\nu, q^2) &= \sum_n \langle 0 | j^\mu(0) | \bar{P}, n \rangle_c \langle \bar{P}, n | j^\nu(0) | 0 \rangle_c (2\pi)^3 \delta^4(q - P - p_n) \\
 &= \frac{1}{m^2} \bar{W}_2(\nu, q^2) \left(P^\mu - \frac{P \cdot q}{q^2} q^\mu \right) \left(P^\nu - \frac{P \cdot q}{q^2} q^\nu \right) \\
 &\quad + \bar{W}_1(\nu, q^2) \left(-g^{\mu\nu} + \frac{q^\mu q^\nu}{q^2} \right) \tag{2.5c}
 \end{aligned}$$

for 2.1(a), 2.1(b), and 2.1(c)¹⁶ respectively. In Eqs. 2.5(b) and 2.5(c) the subscript c denotes the connected part.

The mere fact that we have used variables of the same name and a common plot to describe three different physical processes does not in itself imply any relations between the processes. Some relations which do exist follow from crossing and analyticity as we now spell out.

Consider the non-forward, spin-averaged, virtual Compton amplitude

$$T^{\mu\nu}(\nu, t, q_1^2, q_2^2) = i \int d^4x e^{i(q_1+q_2) \cdot \frac{x}{2}} \langle p_2 | T(j^\mu(\frac{x}{2}), j^\nu(-\frac{x}{2})) | p_1 \rangle_c \quad (2.6)$$

which is illustrated in Fig. 3. In Eq. (2.6)

$$\nu = \frac{(s-u)}{4m} = \frac{(p_1+p_2) \cdot (q_1+q_2)}{4m}$$

$$s = (p_1 + q_1)^2,$$

$$u = (p_1 - q_2)^2,$$

and

$$t = (q_1 - q_2)^2.$$

This Compton amplitude for $t < 0$ (aside from anomalous singularities^{14,17}) is expected to be an analytic function of ν , q_1^2 and q_2^2 . One expects both right (s channel) and left (u channel) hand cuts in ν and right hand cuts in q_1^2 and q_2^2 .

The substitution law along with the charge conjugation property $j^\mu = -C j^\mu C^{-1}$ gives the crossing symmetry property,

$$T^{\nu\mu}(-\nu, t, q_2^2, q_1^2) = T^{\mu\nu}(\nu, t, q_1^2, q_2^2). \quad (2.7)$$

After imposing current conservation one finds (as in Eq. (2.5a)) that the spin averaged amplitude is automatically symmetric in the indices μ and ν at $t=0$.

The discontinuities which correspond to the physical observables 2.5(a) - 2.5(c) are

$$T^{\mu\nu}(\nu+i\epsilon, 0, q^2, q^2) - T^{\mu\nu}(\nu-i\epsilon, 0, q^2, q^2) = 2i W^{\mu\nu}(\nu, q^2) \quad (2.8a)$$

with $\nu > 0$, $q^2 < 0$,

$$\begin{aligned} T^{\mu\nu}(\nu+i\epsilon, 0, q^2 + i\epsilon', q^2 - i\epsilon'') - T^{\mu\nu}(\nu-i\epsilon, 0, q^2 + i\epsilon', q^2 - i\epsilon'') \\ = 2i \tilde{W}^{\mu\nu}(\nu, q^2) \end{aligned} \quad (2.8b)$$

with $\nu > 0$, $q^2 > 0$, and

$$\begin{aligned} T^{\mu\nu}(\nu+i\epsilon, 0, q^2 + i\epsilon', q^2 - i\epsilon'') - T^{\mu\nu}(\nu-i\epsilon, 0, q^2 + i\epsilon', q^2 - i\epsilon'') \\ = 2i \bar{W}^{\mu\nu}(\nu, q^2) \end{aligned} \quad (2.8c)$$

with $\nu < 0$, $q^2 > 0$, respectively. We illustrate the discontinuity equations 2.8(a) - 2.8(c) in Fig. 4. The normal threshold cuts in ν begin at $\nu_R = +v_0$ and $\nu_L = -v_0$ where

$$2m v_0 = (m + \mu)^2 - m^2 - q^2 + i(\epsilon' + \epsilon''), \quad (2.9)$$

corresponding to single meson production.

We note that for the space-like case ($q^2 < 0$) appropriate to inelastic scattering (2.1a) the right and left hand cuts are non-overlapping as shown in Fig. 5(a). For the time-like cases ($q^2 > 0$), Figs. 5(b) and 5(c), the cuts are overlapping and one must take care to circle only the right hand branch point at $+v_0$ when taking the discontinuities in Eqs. (2.8b) and Eqs. (2.8c).

By inspection of Eqs. (2.8a) and (2.8c) along with Fig. 2 we see a convenient way to analytically continue from inelastic scattering to the annihilation region: continue in the virtual photon masses from space-like to time-like values keeping s fixed at a positive and

physical value. It is clear, however, that it is necessary to distinguish the initial and final photon masses q_1^2 , q_2^2 respectively in order that one may continue q_1^2 above its cut ($+i\epsilon$) and q_2^2 below its cut ($-i\epsilon$). In the process of continuation we pass through the three body annihilation region; the prescription given is correct for this region also - Eq. (2.8b).

In addition to the three (s-channel) discontinuities which we have been discussing there are three additional (u-channel) discontinuities of the virtual Compton amplitude which describe similar physical processes.

$$T^{\nu\mu}(\nu-i\epsilon, 0, q^2, q^2) - T^{\nu\mu}(\nu+i\epsilon, 0, q^2, q^2) = 2i W_C^{\nu\mu}(\nu, q^2) \quad (2.10a)$$

with $\nu < 0$, $q^2 < 0$,

$$\begin{aligned} T^{\nu\mu}(\nu-i\epsilon, 0, q^2-i\epsilon, q^2+i\epsilon) - T^{\nu\mu}(\nu+i\epsilon, 0, q^2-i\epsilon, q^2+i\epsilon) \\ = 2i \tilde{W}_C^{\nu\mu}(\nu, q^2) \end{aligned} \quad (2.10b)$$

with $\nu < 0$, $q^2 > 0$, and

$$\begin{aligned} T^{\nu\mu}(\nu-i\epsilon, 0, q^2-i\epsilon, q^2+i\epsilon) - T^{\nu\mu}(\nu+i\epsilon, 0, q^2-i\epsilon, q^2+i\epsilon) \\ = 2i \bar{W}_C^{\nu\mu}(\nu, q^2) \end{aligned} \quad (2.10c)$$

with $\nu > 0$, $q^2 > 0$.

The corresponding physical processes are obtained from those listed in Eqs. (2.1a) - (2.1c) by the substitution $H \leftrightarrow \bar{H}$. The corresponding physical regions are obtained by reflecting the regions in Fig. 2 about the q^2 axis; see Fig. 6. The crossing property, Eq. (2.11), shows immediately that the cross sections for the latter processes ($e^- + \bar{H} \rightarrow e^- + \bar{X}$, $e^- + e^+ + \bar{H} \rightarrow \bar{X}$, and $e^- + e^+ \rightarrow \bar{H} + \bar{X}$) are identical to those for 2.1(a) - 2.1(c) respectively. Note that certain regions

of the q^2, ν plane are inhabited by two different physical processes. This does not imply that the rates for the two processes are equal since they are given by different discontinuities of the same master analytic function (e.g. in general $\tilde{W}_c^{\nu\mu} \neq \tilde{W}^{\mu\nu}$.)

Finally we consider the Bjorken scaling limit. For all processes we define a scaling variable¹⁹

$$\omega = x^{-1} = 2m \nu / (-q^2) \quad (2.11)$$

and consider the limit $|q^2| \rightarrow \infty$, ω fixed. Furthermore in the Bjorken limit one imposes the additional restriction $m_x^2 \gg m^2$. For annihilation therefore

$$(2 \sqrt{\frac{m^2}{q^2}}) \leq \omega \leq 1 - O\left(\frac{m^2}{q^2}\right) \quad (2.12)$$

and for inelastic scattering

$$1 + O\left(\frac{m^2}{-q^2}\right) \leq \omega \leq O\left(\frac{-q^2}{m^2}\right). \quad (2.13)$$

We pick scaling functions in the standard way.

For inelastic scattering (recall $\nu > 0$)

$$F_1(\omega) \equiv \lim_{-q^2 \rightarrow \infty} [m W_1(\nu, q^2)] \quad (2.14)$$

ω fixed

and

$$F_2(\omega) \equiv \lim_{-q^2 \rightarrow \infty} [\nu W_2(\nu, q^2)]. \quad (2.15)$$

ω fixed

A convenient combination is

$$F_L(\omega) \equiv F_1(\omega) - 1/2 \omega F_2(\omega). \quad (2.16)$$

In the region $\omega > 1$ one has the condition $F_1, F_L \geq 0$, which follows from the positivity of the cross section. The Callan-Gross relation²⁰ for theories which scale is $F_L = 0$ ($F_1 = 0$) for currents built entirely from spin 1/2 (spin 0) fields.

For annihilation (recall $\nu < 0$)

$$\bar{F}_1(\omega) \equiv \lim_{q^2 \rightarrow \infty} [m \bar{W}_1(\nu, q^2)] \quad (2.17)$$

ω fixed

and

$$\bar{F}_2(\omega) \equiv \lim_{q^2 \rightarrow \infty} [-\nu \bar{W}_2(\nu, q^2)]. \quad (2.18)$$

ω fixed

Again it is useful to consider a combination

$$\bar{F}_L(\omega) \equiv \bar{F}_1(\omega) + 1/2 \omega \bar{F}_2(\omega). \quad (2.19)$$

As in inelastic scattering one has a positivity condition $\bar{F}_1, \bar{F}_L \geq 0$ valid for $0 < \omega < 1$. Also $\bar{F}_L = 0$ ($\bar{F}_1 = 0$) in scaling theories with a current built from spin 1/2 (spin 0) fields exclusively. [Note the sign difference between the definitions (2.16) and (2.19).]

For completeness we recall the annihilation cross section in the center-of-mass system (Bjorken limit)

$$\frac{d^2 \bar{\sigma}}{d\omega d \cos \theta} = \frac{\pi \alpha^2 \omega}{q^2} [\bar{F}_1(\omega) (1 + \cos^2 \theta_c) + \bar{F}_L(\omega) (1 - \cos^2 \theta_c)] \quad (2.20)$$

showing the characteristic angular dependence for currents built from spin 1/2 or spin 0 fields.

III. Perturbation Theory Results

In this section we identify and calculate those diagrams in the neutral vector gluon model (massive QED) which make leading contributions in the Bjorken limit to the inclusive annihilation process $e^- + e^+ \rightarrow \bar{P} + X$. Previous calculations^{1,3} of inelastic scattering in the neutral vector gluon model, as well as scattering and annihilation calculations in γ_5 and other field theories,⁵⁻¹¹ enable one to anticipate that Bjorken scaling will be broken by the presence of $\ln q^2$ terms. This occurs because massive QED is a renormalizable but not a superrenormalizable theory.

A complete calculation of all terms which survive in the Bjorken limit is hopelessly difficult. In all our work we make a leading-logarithm approximation. Namely, in each order of perturbation theory we compute those terms with the highest power of $\ln q^2$ and then sum the result to all orders in perturbation theory.

It should be emphasized that here, as in our previous work, we make the leading-logarithm approximation for each exclusive channel n , $e^- + e^+ \rightarrow \bar{P} + n$. We then compute the inclusive process $e^- + e^+ \rightarrow \bar{P} + X$ by summing the result over n .

Theoretical calculations can also be carried out using a different leading-logarithm approximation. Namely one can first form the inclusive cross-section by summing over n and only then in each order of perturbation theory make a leading-logarithm approximation. Obviously one should compare results from the different leading-logarithm approximations only in those domains of common applicability. A detailed discussion of this and related matters has already been given in Sec. III of II. Let us,

however, briefly remind the reader that the leading logarithm approximation which we use picks out a well defined set of diagrams which in fact contain the key difference between the neutral vector and the neutral (pseudo) scalar models. Moreover the sum of the terms which we calculate has an acceptable analytic form (no ghost cuts or singularities) and a simple physical interpretation.

A convenient frame for the annihilation calculation is

$$P = (1, \vec{0}, m^2) \quad (3.1)$$

$$q = (\omega^{-1}, \vec{0}, q^2\omega) \quad (3.2.)$$

where we have used the (+, \perp , -) notation for four vectors $[(v^+, \vec{v}, v^-) = (v^0 + v^3, v^1, v^2, v^0 - v^3)]$. Recall also from Sec. II, $mv = -P \cdot q < 0$, $\omega = 2mv/(-q^2) > 0$.

Labelling of the additional emitted particles is as follows. The leading diagrams contain no additional fermion-antifermion pairs besides the one required to produce the detected antifermion. We call the accompanying fermion P' ,

$$P' = (u', \vec{p}', P'^-) = (u', \vec{p}', \frac{m^2 + \vec{p}'^2}{u'}). \quad (3.3)$$

Emitted neutral vector mesons are labelled by

$$k_i = (u_i, \vec{k}_i, k_i^-) = (u_i, \vec{k}_i, \frac{u_i^2 + \vec{k}_i^2}{u_i}). \quad (3.4.)$$

In this frame we pick out the structure functions as follows:

$$\frac{1}{\pi} \bar{W}^{11} = \frac{1}{m} \bar{F}_T(v, q^2) \quad (3.5.)$$

$$\frac{1}{\pi} \bar{W}^{--} = q^2 \omega^2 \frac{1}{m} \bar{F}_L(v, q^2). \quad (3.6)$$

A. Born Term

For the Born diagram, Fig. 7, one has

$$\bar{F}_1^B = \frac{1}{2} \delta(1-\omega) \quad (3.7)$$

$$\bar{F}_L^B = 0. \quad (3.8)$$

Even for this simple diagram it is possible to find some insights into the approximations which are valid in higher orders. According to Eq. (3.5)

$$\bar{F}_1^B = \frac{1}{4} \int \frac{du' d^2P'}{u'} \delta\left(\frac{1}{\omega} - 1 - u'\right) \delta^2(\vec{P}') \\ \times \delta(q^2\omega - m^2 - \frac{\vec{P}'^2 + m^2}{u'}) \text{Tr}[(\not{P}' - m) \gamma^1 (\not{P}' + m) \gamma^1]. \quad (3.9)$$

The trace is easily evaluated and equals

$$4 \left(\frac{1}{2} P'^- + \frac{1}{2} m^2 u' + m^2 \right)$$

from which it trivially follows that

$$\bar{F}_1^B = \left(\frac{1}{2} P'^- + \frac{1}{2} m^2 u' + m^2 \right) \delta\left(\frac{1}{\omega} - 1\right) (q^2\omega)^{-1} \quad (3.10)$$

where $u' = m^2/(q^2\omega)$, $P'^- = m^2/u' = q^2\omega$. Thus dropping $O(1/q^2)$ terms one obtains Eq. (3.7).

We see that P'^- was $O(q^2)$ while P'^+ = $O(1/q^2)$. This result generalizes to more complicated diagrams as follows. The + momentum brought in by q predominantly follows the P (antiproton) line and the momentum predominantly follows the P' (proton) line.

Let us turn now to higher order diagrams. In what follows we shall reserve more detailed calculations for Appendix A and present only the results and salient approximations in this section. As we mentioned above we can lean heavily on our previous work on inelastic scattering

in the vector gluon model.

B. One Meson Production

Diagrams with one meson in the intermediate state are of the three main types shown in Fig. 8. Fig. 8(a) is analogous to the "outer rainbow" or ladder diagram for inelastic scattering. We found in I that these diagrams, although leading in γ_5 theory, are non leading in massive QED. The same is true for annihilation. We see from Eq. (A.5) that the structure function corresponding to Fig. 8(a) contains a single power of $\ln q^2$ with no potential for further powers of $\ln q^2$ upon integration over ω . This is typical of all outer rainbow diagrams. They form a simple exponential series in $e^2 \ln(q^2/\mu^2)$, the logarithms arising from ultraviolet values of the transverse momenta, $\vec{k}_i^2 \leq \epsilon q^2$. In fact, as in the scattering case, the result for the outer rainbow diagrams can be obtained simply from the γ_5 annihilation result by the replacement $g^2 \rightarrow 2e^2$. [g is the coupling constant in γ_5 theory, e the coupling in the vector theory.] The rainbow diagrams are leading in the γ_5 theory.

Fig. 8(b) is the analog of the "inner rainbow" diagrams of inelastic scattering. Again in the vector theory they are non-leading and form an exponential series in $\ln q^2$ which can be obtained from the γ_5 annihilation result by $g^2 \rightarrow 2e^2$.

Fig. 8(c) is the diagram (plus its mirror image) which makes the leading contribution in $O(e^2)$ to the annihilation structure functions for the one meson production channel. It is the simplest member of the class of leading diagrams and is analogous to the "inner-outer" diagrams

we found important for inelastic scattering. From Eq. (A.9) ($\lambda \equiv e^2/16\pi^2$)

$$\bar{F}_1^{8(c)}(\omega, \ln q^2) = \lambda(1-\omega)^{-1} \ln \left[\frac{q^2(1-\omega)}{\mu^2} \right]. \quad (3.11)$$

valid for $1 > 1-\omega \gg (\mu^2/q^2)$. The presence of the $(1-\omega)^{-1}$ factor in Eq. (3.11) enhances the region $\omega \sim 1$ and can give a further logarithm upon integration over ω . In obtaining Eq. (3.11) one may neglect k_i^- additively compared to $P_i^- \approx q^2\omega$. The logarithm comes from a transverse momentum integration; in higher order diagrams of this class one also picks up logarithms from longitudinal integrations.

C. Two Meson Production

Consider next the leading contributions to two meson productions which come from the diagrams in Fig. 9(a) and 9(b). Their sum, from Appendix A, is

$$\bar{F}_1^{9(a)+9(b)}(\omega, \ln q^2) = \lambda^2(1-\omega)^{-1} \ln^3 \left[\frac{q^2(1-\omega)}{\mu^2} \right]. \quad (3.12)$$

We see that compared to Eq. (3.11) one has gained two powers of $\ln q^2$ at the price of a single power of λ . By contrast the $O(\lambda^2)$ generalizations of Figs. 8(a) and 8(b) only increase by a single additional power of $\ln q^2$ and thus are non-leading by our rules.

As we discuss in Appendix A, considerable simplifications occur if one combines the expressions for 8(a) and 8(b) before carrying out the phase space integrations. After a more difficult calculation one finds that diagrams 9(a) and 9(b) separately contribute ($g^{\mu\nu}$ gauge) $2/3$ and $1/3$ respectively of the answer quoted in Eq. (3.12). The fact that the graphs combine to a simple eikonal-like result is completely characteristic of massive QED. In particular we note that the $\omega \sim 1$ enhancement

is a result of the (approximately) freely propagating antifermion; the $(1-\omega)^{-1}$ factor can be directly traced to the $(P-q)^2-m^2$ pole term in diagrams 9(a) and 9(b).

D. General Case

Having identified the class of leading diagrams we calculate the general case for the production of n mesons in $O(\lambda^n)$. The leading diagrams are the obvious generalizations of Figs. 9(a) and 9(b) and are represented by Fig. 10. The shaded box is meant to indicate the summation over all permutations of attachment of the vector meson lines. As expected on the basis of remarks above and our work in I, after summing over all such permutations of the meson attachments one obtains a simple, eikonal-like result.

Namely when the two groups of vector mesons in Fig. 10 contain r and ℓ particles, $r+\ell=n$, we find

$$\bar{F}_1^{(\ell, r)}(\omega, \ln q^2) = \lambda^n \frac{1}{1-\omega} \frac{\ell+r}{\ell!r!} \left[\frac{\ln q^2(1-\omega)}{\mu^2} \right]^{2n-1}. \quad (3.13)$$

The integration regions which are important for Eq. (3.13) are as follows. Label the two groups of vector mesons with and without primes. We pick up n ultraviolet logarithms from transverse integrations over the regions

$$\vec{k}_i^2 \leq \epsilon q^2 \omega u_i \quad (3.14)$$

$$\vec{k}'_i{}^2 \leq \epsilon' q^2 \omega u'_i \quad (3.14')$$

and $n-1$ infrared logarithms from integration over longitudinal momenta.

The important regions for the latter next according to

$$\frac{1}{\varepsilon} \frac{\mu^2}{q^2} \leq u_i \leq \varepsilon u_{i-1}, \quad i \neq 1 \quad (3.15)$$

$$\frac{1}{\varepsilon'} \frac{\mu^2}{q^2} \leq u_j' \leq \varepsilon' u_{j-1}' \quad j \neq 1. \quad (3.15')$$

The final integrals over u_1 and u_1' break into the sum of two terms. One is integrated $\frac{\mu^2}{\eta q^2} \leq u_1' \leq \varepsilon u_1$ with u_1 fixed by the delta function $u_1 = 1-\omega$; for the other let $u_1 \leftrightarrow u_1'$. [See the discussion above Eq. (4.17) in I.]

Summing the result given in Eq. (3.13) over all allowed values of l, r consistent with $l+r=n$ = fixed gives

$$\bar{F}_1^{(n)'} = 2\lambda \frac{1}{(1-\omega)} \ln \left[\frac{q^2(1-\omega)}{\mu^2} \right] \frac{1}{(n-1)!} \left(2\lambda \ln^2 \left[\frac{q^2(1-\omega)}{\mu^2} \right] \right)^{n-1}. \quad (3.16)$$

Eq. (3.16) is not the final result for intermediate states with n mesons along with the proton-antiproton pair. It is only the contribution from the lowest order in the coupling, namely $O(\lambda^n)$, which can contribute to n meson production. For fixed n and higher order in λ one has vertex and self energy corrections to the order λ^n diagrams. We shall not go through an explicit study as we did in the inelastic scattering case since the techniques are so similar. Instead let us merely state the obvious and analogous results.

The leading diagrams are of the type shown in Fig. 11. The shaded boxes stand for the sum over all permutations of real and virtual meson emission (absorption) as is characteristic of a gauge invariant vector theory. To leading logarithmic accuracy interactions between the meson lines can be neglected.

After evaluating the leading contribution of the sum of all graphs

of the type shown in Fig. 11 one finds a simple result. The result is the lowest order result, Eq. (3.13) or Eq. (3.16), multiplied by the absolute square of $\bar{\mathcal{F}}_1(q^2)$. $\bar{\mathcal{F}}_1(q^2)$ is the elastic form factor evaluated to leading logarithmic accuracy in the time-like limit $q^2 \rightarrow \infty$. For the space-like limit $q^2 \rightarrow -\infty$ one has³ to leading logarithmic accuracy

$$\bar{\mathcal{F}}_1(q^2) \xrightarrow{-q^2 \rightarrow \infty} \exp(-\lambda \ln^2[-q^2/\mu^2]). \quad (3.17)$$

Since

$$\ln(-q^2 \pm i\epsilon) = \ln|q^2| \mp i\pi,$$

we have

$$\begin{aligned} \bar{\mathcal{F}}_1(q^2)^* \bar{\mathcal{F}}_1(q^2) &= \exp(-2\lambda \ln^2[q^2/\mu^2] + 2\lambda \pi^2) \\ &= \exp(-2\lambda \ln^2[q^2/\mu^2]) \end{aligned}$$

to leading-logarithmic accuracy. Thus our final result summed to all orders in the coupling for n meson intermediate states is

$$\begin{aligned} \bar{\mathcal{F}}_1^{(n)}(\omega, \ln q^2) &= 2\lambda \frac{1}{(1-\omega)} \ln \left[\frac{q^2(1-\omega)}{\mu^2} \right] \exp(-2\lambda \ln^2 \left[\frac{-q^2}{\mu^2} \right]) \\ &\quad \times \frac{1}{(n-1)!} (2\lambda \ln^2 \left[\frac{q^2(1-\omega)}{\mu^2} \right])^{n-1}. \end{aligned} \quad (3.18)$$

Such a simple result for the higher order radiative corrections naturally has a simple interpretation. We see from Eqs. (3.14), (3.14'), (3.15), and (3.15') that the produced vector mesons have transverse momenta small compared to q^2 and small longitudinal (+) momentum fractions. Therefore the proton-antiproton pair produced by the external current are quite close to their mass shells. Hence it is quite plausible that the elastic form factor enters.

The result given in Eq. (3.18) forms a simple exponential series which is easily summed over n ,

$$\bar{F}_1(\omega, \ln q^2) = 2\lambda \frac{1}{(1-\omega)} \ln \left[\frac{q^2(1-\omega)}{\mu^2} \right] \\ \times \exp \left(2\lambda \ln^2 \left[\frac{q^2(1-\omega)}{\mu^2} \right] - 2\lambda \ln^2 \left[\frac{q^2}{\mu^2} \right] \right). \quad (3.19)$$

We note that the presence of the elastic form factor correction in Eq. (3.19) provides strong damping at large q^2 which compensates the growth due to real vector meson production - the sum over n . This is physically sensible and necessary and leads to a well behaved total cross section as $q^2 \rightarrow \infty$.

In particular we note that there is an explicit cancellation of the $\ln^2[q^2/\mu^2]$ term in the exponent of Eq. (3.19) leaving as the exponent $2\lambda \ln[q^2/\mu^2] \ln(1-\omega) + \lambda \ln^2(1-\omega)$. This means that for the inclusive quantity \bar{F}_1 , in contrast to the exclusive quantities $\bar{F}_1^{(n)}$, the inner-outer diagrams we consider form a series in single powers of $\ln q^2$. This, as we remarked above, is origin of the difference between the leading-log approximation we employ and that of Ref. (8). The cancellation of real and virtual meson processes has its origin in the same mechanism that underlies the infrared region for photons in massless QED.

It remains to calculate \bar{F}_2 by, say, evaluating the $u=v(-)$ component of $\bar{W}^{\mu\nu}$; see Eq. (3.6). Again we spare the reader a tedious repetition of a similar calculation in II for inelastic scattering. The result is

$$\bar{F}_2(\omega, \ln q^2) \doteq -(2/\omega) \bar{F}_1(\omega, \ln q^2) \quad (3.20)$$

or equivalently

$$\bar{F}_L(\omega, \ln q^2) \doteq 0. \quad (3.21)$$

where \doteq stands for equality to leading-logarithmic accuracy.

E. Distribution Properties and Integrals

We conclude this section on some of the properties of the final states which build up the structure function $\bar{F}_1(\omega)$ in Eq. (3.19).

The average number of emitted antiprotons is a constant equal to one since our leading diagrams contain just a single fermion - antifermion loop. This is because in annihilation, as for inelastic scattering, for a given total multiplicity of fermions plus mesons, diagrams with additional fermion-antifermion pairs, either from closed loops or from Z graphs, are smaller by at least a logarithm in each order of perturbation theory than the diagrams illustrated in Fig. 11.

As a check on our results let us compute the fermion multiplicity $n(\bar{P})$ by integrating over the inclusive cross section.

$$\begin{aligned} \langle\langle n(\bar{P}) \rangle\rangle &= (\bar{\sigma})^{-1} \left\{ \int d\Omega \int_0^1 d\omega \frac{d^2 \bar{\sigma}}{d\Omega d\omega} \right\} \\ &= \int_{\frac{1}{\epsilon} \frac{\mu^2}{q^2}}^1 d\omega \omega^2 \bar{F}_1(\omega) \\ &= \frac{1}{\epsilon} \int_{\sqrt{q^2}}^{\mu^2} \frac{d\omega}{\omega} \end{aligned} \quad (3.22)$$

where we have used Eq. (2.20) and used the leading logarithm result $\bar{F}_L(\omega) \doteq 0$. Using Eq. (3.19) the integral in Eq. (3.22) is easily carried out:

$$\langle\langle n(\bar{P}) \rangle\rangle \doteq 1. \quad (3.23)$$

Note that this integral is just the sum rule quantity Σ_2 defined by Eq. (6.2) of I.

Similarly one can calculate the fraction $\langle \omega(\vec{P}) \rangle$ of the center of mass energy $\sqrt{q^2}$ which is given to antiprotons

$$\langle \langle \omega(\vec{P}) \rangle \rangle = \frac{\int_0^1 \frac{1}{\epsilon} \frac{\mu^2}{q^2} \omega^2 2\bar{F}_1(\omega) d\omega}{\frac{1}{\epsilon} \sqrt{\frac{\mu^2}{q^2}}} \doteq 1 \quad (3.24)$$

This second integral is recognized as the quantity Σ_1 defined in Eq. (6.1) of I. The fact that the quantities $\langle \langle n(\vec{P}) \rangle \rangle$ and $\langle \langle \omega(\vec{P}) \rangle \rangle$ are independent of q^2 even though the structure function \bar{F}_1 itself does not scale is an interesting and non-trivial result.

We turn now to the properties of the mesons which accompany the photon-antiproton pair. The multiplicity of produced vector mesons for fixed ω is

$$\begin{aligned} \langle n(\text{vm}) \rangle &= \left(\sum_n n \bar{F}_1^{(n)} \right) / \left(\sum_n \bar{F}_1^{(n)} \right) \\ &\approx 2\lambda \ln^2 \left[\frac{q^2(1-\omega)}{\mu^2} \right]. \end{aligned} \quad (3.25)$$

Similarly the spread in average number also grows like $\ln^2 q^2$,

$$\langle n(\text{vm}) \rangle^2 - \langle n(\text{vm}) \rangle = \langle n(\text{vm}) \rangle. \quad (3.26)$$

Eqs. (3.25 and (3.26) are, of course, a simple consequence of the Poisson nature of the distribution in n which is manifest in Eq. (3.18). This Poisson structure reflects the fact that in the leading logarithm domain in which we work one has, after summation over all diagrams of the type shown in Fig. 11, independent, uncorrelated emission of vector

mesons, and hence an eikonal type result.

The average energy fraction of the vector mesons, already known to be small by Eq. (3.24), is

$$\begin{aligned} \langle\langle(1-\omega)\rangle\rangle &= (\int d\omega (1-\omega)\omega \bar{F}_1) / (\int d\omega \omega \bar{F}_1) \\ &= O(\mu^2/q^2) \end{aligned} \quad (3.27)$$

which reflects the strong peaking of \bar{F}_1 near $\omega=1$.

It is easy to see from Eqs. (3.14), (3.14'), (3.15), and (3.15') that in the center-of-mass system the vector mesons arrange themselves in two cones around the proton-antiproton direction. The individual vector mesons in the cones are characterized by opening angles

$$\tan \theta_i = \epsilon(u_i)^{-1/2} \quad (3.28)$$

as in I. [See, too, Fig. 8 in I.]

The average transverse momentum of a vector meson with respect to its "parent" fermion is

$$\langle \vec{k}^2 \rangle = \epsilon q^2 (1-\omega) / (\ln [\frac{q^2(1-\omega)}{\mu^2}]). \quad (3.29)$$

Thus on average the transverse momentum grows linearly with q^2 except in the threshold region $(1-\omega) = O(\mu^2/q^2)$. This growth reflects the absence of a transverse momentum cutoff in perturbation theory and undermines Bjorken scaling.

IV. Reciprocal Relation and Analytic Continuation

In this section we discuss the relations which hold between our leading-logarithmic approximations to the structure functions. For convenience we will continue to discuss the spin 1/2 theory for which $F_L = \bar{F}_L \doteq 0$. Essentially identical results hold for spin 0 nucleons (massive scalar electrodynamics).

A. Analytic Continuation

In a scaling theory the statement that the annihilation structure function is the analytic continuation in ω of the inelastic scattering structure function implies

$$-\bar{F}_1(\omega) = F_1(\omega) . \quad (4.1)$$

[The minus sign in Eq. (4.1) is purely conventional. Note that the positivity conditions mentioned in Sec. II only apply in the physical regions of \bar{F}_1 and F_1 .] Eq. (4.1) has the following interpretation. One first evaluates $\lim (m W_1(\nu, q^2)) \equiv F_1(\omega)$ in the Bjorken limit with $\omega > 1$ and then analytically continues the result to values $0 < \omega < 1$ and compares to $\bar{F}_1(\omega)$. Naturally if one evaluates $\lim(m W_1(\nu, q^2))$ for $\omega < 1$ the result is trivially zero; this, however, is irrelevant to the continuation of $F_1(\omega)$.

As discussed in Sec. II the continuation is conveniently done along the path $s = \text{const.}$ Therefore since $\omega = s/(-q^2) + 1$ as ω varies we may expect to encounter singularities in q^2 . When this happens, as discussed in Sec. II, we must separate $q^2 \rightarrow q_1^2, q_2^2$ and go around the q_1^2, q_2^2 singularities in complex conjugate ways. One must therefore introduce twin scaling variables $\omega_1 = s/(-q_1^2) + 1$ and $\omega_2 = s/(-q_2^2) + 1$ and interpret Eq. (4.1) as

$$-\bar{F}_1(\omega) = \lim_{\varepsilon \rightarrow 0} F_1(\omega_1 = \omega + i\varepsilon, \omega_2 = \omega - i\varepsilon), \quad (4.2)$$

where on the right hand side the limit is taken after the continuation is performed.

In renormalizable field theories which characteristically break strict Bjorken scaling because of $\ln q^2$ structure one clearly encounters singularities in q^2 during the continuation from scattering to annihilation. Let us now study this explicitly in the vector gluon model.

So far we have not distinguished the initial (q_1^2) and final (q_2^2) photon masses in our work. It is easy to see, however, that the scattering function

$$F_1(\omega, \ln(-q^2)) = \frac{2\lambda}{\omega-1} \ln \left[\frac{-q^2(\omega-1)}{\mu^2} \right] \\ \times \exp \left\{ 2\lambda \ln^2 \left[\frac{-q^2(\omega-1)}{\mu^2} \right] - 2\lambda \ln^2 \left[\frac{-q^2}{\mu^2} \right] \right\} \quad (4.3)$$

computed in I for $q^2 < 0$, $\omega > 1$ is more properly written

$$F_1 = \frac{2\lambda}{\omega-1} \ln \left[\frac{s}{\mu^2} \right] \exp \left\{ 2\lambda \ln^2 \left[\frac{s}{\mu^2} \right] - \lambda \ln \left[\frac{-q_1^2}{\mu^2} \right] - \lambda \left[\frac{-q_2^2}{\mu^2} \right] \right\} \quad (4.4)$$

where $s = -q_1^2(\omega_1-1) = -q_2^2(\omega_2-1)$, aside from $0(m^2/q^2)$ corrections.

In Eq. (4.4) all logarithms are real for $s > 0$, $-q_1^2 > 0$, $-q_2^2 > 0$. Similarly in place of Eq. (3.19) one ought to write

$$\bar{F}_1 = \frac{2\lambda}{1-\omega} \ln \left[\frac{s}{\mu^2} \right] \exp \left\{ 2\lambda \ln^2 \left[\frac{s}{\mu^2} \right] - \lambda \ln^2 \left[\frac{q_1^2}{\mu^2} \right] - \lambda \ln^2 \left[\frac{q_2^2}{\mu^2} \right] \right\} \quad (4.5)$$

where all logarithms are real for $s, q_1^2, q_2^2 > 0$.

In the continuation of Eq. (4.4) to time-like photon masses the correct phase choices are

$$\begin{aligned}
\ln \left(\frac{-q_1^2}{\mu^2} \right) &\rightarrow \ln \left(\frac{q_1^2}{\mu^2} \right) - i\pi \\
\ln \left(\frac{-q_2^2}{\mu^2} \right) &\rightarrow \ln \left(\frac{q_2^2}{\mu^2} \right) + i\pi
\end{aligned} \tag{4.6}$$

Therefore dropping $-\pi^2$ compared to $\ln^2[q^2/\mu^2]$ we see that the analytic continuation condition is satisfied. [It might be argued that in leading logarithm calculations one may neglect $\pm i\pi$ compared to $\ln[|q^2|/\mu^2]$, and hence one need not be concerned with $i\epsilon$ prescriptions. Such an attitude is improper, however, since the neglected next-to-leading logarithmic powers are real and therefore cannot cancel spurious imaginary terms which arise if the branch points are not circumvented properly.]

B. Reciprocal Relation

Putting aside matters of analytic continuation we see by inspection that Eqs. (3.19) and (4.3) are connected by a reciprocal relation

$$\bar{F}_1(\omega, \ln q^2) \doteq +\frac{1}{\omega} F_1\left(\frac{1}{\omega}, \ln(-q^2)\right). \tag{4.7}$$

To establish Eq. (4.7) we must make the approximation

$$\begin{aligned}
\ln \left[\frac{-q^2}{\mu^2} \left(\frac{1}{\omega} - 1 \right) \right] &= \ln \left[\frac{-q^2(1-\omega)}{\mu^2} \right] - \ln(\omega) \\
&\doteq \ln \left[\frac{-q}{\mu^2} (1-\omega) \right].
\end{aligned} \tag{4.8}$$

This approximation is acceptable within our leading-log philosophy since even though we have treated $\ln(q^2/\mu^2)$ and $\ln(\omega-1)$ consistently on the same footing we have not done the same for any $\ln(\omega)$ factors.

This reciprocal relation, first established in the Mellin transform space for the rainbow diagrams in γ_5 theory, was first stated in

the form of Eq. (4.7) by Gribov and Lipatov in their extensive studies of scaling in perturbation theory.⁸ The relation holds on a diagram by diagram basis. For this reason it is unaffected by the fact that the authors of Ref. (8) use a different leading log criterion which picks out a different (wider) set of diagrams than the one we select. It is easy to see by studying low order examples that for a given graph the reciprocal relation, Eq. (4.7), breaks down at a sub-leading² logarithm level. [Recall that the same is true² for the Callan-Gross and other formal light cone-parton model relations.]

Unlike analytic continuation, which cannot be checked experimentally, the reciprocal relation (4.7) connects F_1 in its physical region to \bar{F}_1 in its physical region. It is tempting therefore to abstract the reciprocal relation from its perturbation theory origin and suppose it true for the real world. This is a delicate matter, however, since the reciprocal relation must fail for truly composite systems. [We discuss this further in Sec. VI.]

C. Alternate Technique

In our work so far we have studied the reciprocal relation and the analytic continuation question by actually carrying out all momentum integrations. To extend this study to other classes of diagrams and other theories it is more efficient to use the method we discuss now which allows one to make the comparison at the integrand level after establishing certain approximations.

The method involves only a change of frame for the scattering calculation from the frame of l,

$$F_1^{(12)} = \frac{\lambda}{4\pi} \int_0^{1-\omega^{-1}} dx_1 d^2\ell_1 \frac{(1-\omega^{-1})^2}{x_1(1-\omega^{-1}-x_1)^2} \delta(-q^2\omega-\vec{\ell}_1^2) \frac{(1-\omega^{-1})}{x_1(1-\omega^{-1}-x_1)} . \quad (4.14)$$

After a change of variables $x_1 \rightarrow -u_1$, $\vec{\ell}_1 \rightarrow \vec{k}_1$ in Eq. (4.14) and taking account of an overall sign (a Jacobian factor) because of the delta function, we see $\bar{F}_1^{(8a)}$ and $F_1^{(12)}$ obey the analytic continuation relation, Eq. (4.1).

To see the reciprocal relation perform the scaling

$$x_1 \rightarrow \omega u_1, \quad \vec{\ell}_1^2 \rightarrow \omega^{-1} \vec{k}_1^2 \quad (4.15)$$

in Eq. (4.14). By inspection one then establishes the reciprocal relation, Eq. (4.7).

It is easy to extend this to the general diagram. Using an obvious notation one has

$$F_1 = \prod_{i=1}^N \int \frac{dx_i}{x_i} d^2\ell_i \delta(1-\omega^{-1}-\Sigma x_i) \delta(\Sigma \vec{\ell}_i) \times \delta(-q^2\omega-\Sigma \ell_i^2) f_N(p \cdot \ell_i; \ell_i \cdot \ell_j) \quad (4.16)$$

for inelastic scattering. In Eq. (4.16) the index i runs over all final fermions and mesons. For the corresponding annihilation diagram one has

$$\bar{F}_1 = \prod_{i=1}^N \int \frac{du_i}{u_i} d^2k_i \delta(\omega^{-1}-1-\Sigma u_i) \delta^{(2)}(\Sigma \vec{k}_i) \times \delta(q^2\omega-\Sigma k_i^2) f_N(-p \cdot k_i; k_i \cdot k_j) . \quad (4.17)$$

where i runs over all fermions and mesons which accompany the detected antiproton.

In writing these equations we have neglected mass squared terms in

the dynamical term f . This is appropriate in the Bjorken scaling limit. Mass terms are necessary only to provide cutoffs (scale factors) for logarithmic integrations. After a scale transformation in Eq. (4.14)

$$x_i \rightarrow \omega u_i, \quad \vec{\ell}_i \rightarrow \omega^{-1/2} \vec{k}_i, \quad (4.18)$$

a generalization of Eq. (4.13), direct comparison to Eq. (4.15) shows that the reciprocal relation holds provided

$$f_N(p \cdot \ell_i; \ell_i \cdot \ell_j) \rightarrow \omega^{N-1} f_N(-P \cdot k_i; k_i \cdot k_j) . \quad (4.19)$$

The key point is that after the transformation (4.18) the phase space factors and delta functions in Eqs. (4.16) and (4.17) are identical. [Recall also one changes $-q^2 \rightarrow +q^2$ in the reciprocal relation.] In Appendix B we give an additional example of these scaling techniques.

D. Other Graphs and Other Field Theories.

We have studied in Section III the "inner-outer" graphs, which are the leading graphs in massive QED. This class of graphs satisfied both analytic continuation and the reciprocal relation. In γ_5 theory, which is the other interesting renormalizable theory, these inner-outer graphs are negligible since they are down by $O(q^{-2})$.

Another interesting class of diagrams is the outer rainbow (ladder) graphs. We studied in massive QED a specific example above in part C. Any specific diagram of this type differs from the same diagram in γ_5 by the replacement $g^2 \rightarrow 2e^2$ to leading-logarithmic accuracy. The rainbow graphs has been extensively studied in γ_5 , and both analytic continuation and the reciprocal relation follow. Therefore both follow in massive QED as well. Recall these diagrams represent the leading non-diffractive diagrams in γ_5 theory, and the leading non-diffractive

diagrams in the limit $\omega \rightarrow \infty$ ($\omega \rightarrow 0$) for scattering (annihilation) in massive QED.

A new class of diagrams ("towers") which we now discuss are the leading diffractive (same for proton or neutron targets) graphs in both theories. Figs. 13(a) and 13(b) for γ_5 theory and the analogs 13(c) and 13(d) for QED are the lowest order examples of this class. Figs. 13(a) and 13(b) are explicitly treated in Appendix B. Graphs 13(a) and 13(c) are $O(\lambda^2 \ln^2[-q^2])$ while graphs 13(b) and, in the Feynman gauge, 13(d) are $O(\lambda^2 \ln[-q^2])$. Higher order graphs of the types (a) and (b) form a series in $\lambda^2 \ln^2[-q^2]$ and are therefore as important in the leading log sense as the rainbow graphs. Gribov and Lipatov⁸ and Mason¹⁰ have treated the entire class in detail.

Both relations between inelastic scattering and annihilation obtain for both theories. It is perhaps amusing that these relations also hold for Figs. 13(b) and 13(d), even though they are non-leading. If we can abstract this result, the two relations are properties of the leading behavior of any given graph.

Superrenormalizable theories such as $\lambda\phi^3$ ²² or a cutoff theory such as the Drell, Levy, Yan γ_5 ⁶ theory, are qualitatively different than the renormalizable theories discussed above. This is because their more convergent behavior gives Bjorken scaling.

For the ϕ^3 theory, intuition about momentum flow is a reliable guide to the behavior of any particular diagram. Each additional propagator in an infinite momentum path gives damping by a power of q^2 . This means that diagrams in which the interacting boson propagates freely, as in Fig. 14, lead to $O(q^2)$; form factor corrections to the

external vertices are also absent to $O(q^{-2})$. This simplifies the analyticity properties of the structure function F_L and \bar{F}_L (F_T and \bar{F}_T are zero to $O(q^{-2})$) and analytic continuation follows as previously outlined. The reciprocal relation for F_L and \bar{F}_L is

$$\bar{F}_L(\omega) = +\frac{1}{\omega} F_L(\omega^{-1}), \quad (4.20)$$

or in terms of F_2 ,

$$\bar{F}_2(\omega) = -\omega^{-3} F_2(\omega^{-1}). \quad (4.21)$$

This relation holds in ϕ^3 at least for the ladder diagrams.²³

Cutoff renormalizable field theories, which are non-local, are more complicated, and work is presently in progress on the questions of analytic continuation and the reciprocal relation.

V. Longitudinal Impact Space

In a previous study of scaling in the γ_5 field theory^{5,10} a longitudinal impact parameter (LIP) representation was introduced. This representation was both given a physical interpretation and shown to be convenient for calculations. This section is in two parts. First, we continue the discussion of the physical interpretation of the LIP representation by showing that it is a natural extension of the Regge description of scattering to the Bjorken region. Second, we show how this representation provides a convenient and economic way to study the reciprocal and analytic continuation relations between the deep inelastic and the annihilation structure functions. This discussion is general and is not restricted to perturbation theory.

A. Longitudinal Impact Parameter Representation

We begin with a brief review of the representation itself. We suppress possible explicit dependence on $\ln q^2$ (present in perturbation theory), and without loss of generality, we consider the F_1 and \bar{F}_1 structure functions only. [We drop the subscript 1 throughout this section.] For the scattering process define the transformed structure function $\tilde{F}(\tau)$ by the Mellin transform

$$\tilde{F}(\tau) = \int_0^1 dx x^{\tau-1} F(\omega). \quad (5.1)$$

where $x = 1/\omega$. In the usual definition of the Mellin transform the integral runs from 0 to ∞ . In writing Eq. (5.1) we have integrated only over the physical range of x as is natural.

The inversion formula to Eq. (5.1) is

$$F(\omega) = \int_{c-i\infty}^{c+i\infty} \frac{d\tau}{2\pi i} \omega^\tau \tilde{F}(\tau) \quad (5.2)$$

where c is real and the contour is to the right of all singularities of $\tilde{F}(\tau)$.

That τ is an impact parameter may be seen by analogy to the usual transverse impact parameter b_\perp . First we rewrite Eq. (5.1) as a Laplace transform

$$\tilde{F}(\tau) = \int_0^\infty dz e^{-\tau z} F(e^z) \quad (5.3)$$

where

$$x = e^{-z}.$$

Such a Laplace transform is analogous to the Fourier transforms one writes in the usual eikonal representations with τ playing the role of the impact parameter \vec{b} . This analogy is even sharper if we recall that the two sets of variables

$$(b_1 = E_1/p^+, b_2 = E_2/p^+, \tau = K_3) \quad (5.4)$$

and

$$(p_1, p_2, -z = \ln(p^+/m)). \quad (5.5)$$

form conjugate sets

$$[b_1, p_1] = [b_2, p_2] = [\tau, -z] = -i. \quad (5.6)$$

In Eq. (5.4) K_3 is the generator of boosts in the 3 direction and E_1, E_2 are Euclidean translation operators in the 1, 2 directions. [See Chang and Fishbane, Ref. (10), for details.]

The product $b_i p_i$ appearing in the commutators (5.6) has dimensions of angular momentum. Therefore τz has that same dimension. However, according to (5.5) z is dimensionless, so that τ is itself an angular

momentum.

Now it is clear from Eq. (5.2) that if we push the contour to the left and cross, say, a pole of $\tilde{F}(\tau)$ at $\tau=\alpha$ we will have

$$F(\omega) = \int_{c'-i\infty}^{c'+i\infty} \frac{d\tau}{2\pi i} \omega^\tau \tilde{F}(\tau) + \gamma(\omega)^\alpha \quad (5.7)$$

where γ is the residue of the pole. In the limit $\omega \rightarrow \infty$ the pole term will be the leading part of the amplitude.

Consider now the usual Regge description as applied to the forward virtual Compton amplitude $T^{\mu\nu}(\nu, 0, q^2, q^2)$. The Compton amplitude may be expanded in invariants T_1, T_2 in complete analogy to Eqs. (2.5a)-(2.5c). For simplicity we work only with T_1 and let $T(\nu, q^2) \equiv T_1(\nu, 0, q^2, q^2)$. Recall, by virtue of Eq. (2.7),

$$T(\nu, q^2) = T(-\nu, q^2) \quad (5.8)$$

The standard Froissart-Gribov definition of the positive signature analytically continued t -channel partial wave amplitude is (recall $t=0$)

$$T(j, q^2) = \frac{1}{\pi} \int_{s_0}^{\infty} ds' Q_j \left(1 - \frac{s'}{2m^2} \right) \left\{ \text{disc}_s T(\nu', q^2) + \text{disc}_u T(\nu', q^2) \right\} \quad (5.9)$$

where

$$\text{disc}_u T(-\nu', q^2) = \text{disc}_s T(\nu', q^2) = m W_1(\nu, q^2), \quad (5.10)$$

and

$$\nu' = (s' - m^2 - q^2)/(2m). \quad (5.11)$$

The corresponding Sommerfeld-Watson transformation, after picking up a Regge pole at $j=\alpha$, has the form

$$T(\nu, q^2) = - \int_{C_R^{-i\infty}}^{C_R^{+i\infty}} \frac{d_j}{2i} (2j+1) \frac{\left\{ P_j \left(-1 + \frac{s}{2m^2}\right) + P_j \left(1 - \frac{s}{2m^2}\right) \right\} T(j, q^2)}{2 \sin \pi j} \\ - \pi \beta(q^2) (2\alpha + 1) \frac{\left\{ P_\alpha \left(-1 + \frac{s}{2m^2}\right) + P_\alpha \left(1 - \frac{s}{2m^2}\right) \right\}}{2 \sin \pi \alpha} . \quad (5.12)$$

In the limit $s \rightarrow \infty$, q^2 fixed

$$T(\nu, q^2) = -\pi C_\alpha \beta(q^2) \left(\frac{s}{2m^2}\right)^\alpha \left\{ \frac{e^{-i\pi\alpha} + 1}{\sin \pi\alpha} \right\} + \dots, \quad (5.13)$$

$$C_\alpha = \frac{\Gamma(2\alpha + 2)}{2_\alpha [\Gamma(\alpha+1)]^2} .$$

Therefore

$$\frac{1}{\pi} \text{disc}_s T(\nu, q^2) = C_\alpha \beta(q^2) \left(\frac{s}{2m^2}\right)^\alpha + \dots . \quad (5.14)$$

If we impose Bjorken scaling on Eq. (5.14), in the region $\omega = (s/-q^2)+1 \gg 1$, then the residue function β must have the form²⁴

$$C_\alpha \beta(q^2) = \gamma \left(\frac{2m^2}{-q^2}\right)^\alpha, \quad -q^2 \rightarrow \infty$$

where γ is independent of q^2 . Thus

$$F_1(\omega) = \lim_{\substack{\nu \rightarrow \infty \\ \omega \gg 1}} \left\{ \frac{1}{\pi} \text{disc}_s T(\nu, q^2) \right\} = \gamma(\omega)^\alpha + \dots \quad (5.15)$$

The connection with the longitudinal impact parameter representation of Eq. (5.7) is now obvious. Poles in the variable τ occur at $\tau = \alpha(0)$ where $\alpha(0)$ are the positions at $t=0$ of the even signature Regge poles which can be exchanged in the t -channel of Compton scattering. The residue of the poles in τ space are the Regge pole residues after a $(q^2)^{-\alpha}$ dependence has been factored out. [Strictly speaking since the expansion in Eq. (5.9) is in terms of powers and the expansion in Eq. (5.12) is in terms of Legendre functions, a pole at $\tau = \alpha$ corresponds to a set of

Regge poles at $\tau=\alpha, \alpha-1, \alpha-2, \dots$ and conversely.] The expansion of the inelastic structure function $F(\omega)$ in terms of a few leading poles or cuts in τ is, of course, only relevant to the $\omega \gg 1$ region. This does not prevent us from talking about a LIP representation, Eqs. (5.1) and (5.2), for any value of ω , however.

B. Relations in τ space

In a manner which is completely analogous to what we did in part A we define a transform $\tilde{\tilde{F}}(\tau)$ of the annihilation structure function

$$\tilde{\tilde{F}}(\tau) = \int_0^1 d\omega \omega^{\tau-1} \bar{F}(\omega). \quad (5.16)$$

As we did for scattering, we integrate only over the physical region for annihilation. For annihilation, since $0 < \omega < 1$, there is no $\omega \gg 1$ region where we can think about the dominance of one or a few τ -poles.

One may ask what relation is satisfied by the Mellin transforms $\tilde{\tilde{F}}(\tau)$ and $\tilde{F}(\tau)$ if the analytic continuation relation (4.1) is satisfied. It is obvious without calculation that there is no relation in general since one is integrating $F(\omega)$ over $1 < \omega < \infty$ in Eq. (5.1) and $F(\omega) = \bar{F}(\omega)$ over $0 < \omega < 1$ in Eq. (5.16). We return to this point below, however.

The reciprocal relation (4.7) is a physical region equation so we expect a relation in the LIP space. Using Eq. (4.7),

$$\begin{aligned} \tilde{\tilde{F}}(\tau) &= \int_0^1 d\omega \omega^{\tau-1} \bar{F}(\omega) = \int_0^1 d\omega \omega^{\tau-2} F\left(\frac{1}{\omega}\right) \\ &= \tilde{F}(\tau-1). \end{aligned} \quad (5.17)$$

The converse of this relation is also true. That is, if $\tilde{\tilde{F}}(\tau) = \tilde{F}(\tau-1)$, then the reciprocal relation $\bar{F}(\omega) = \omega^{-1} F(\omega^{-1})$ is satisfied.

As an example consider the outer rainbow (ladder) diagrams in γ_5 theory. These were conveniently calculated in the LIP space and for the $O(g^{2n})$ graph the result was

$$\tilde{F}^{(n)}(\tau) = \frac{1}{2(n!)} \left[\frac{a}{\tau(\tau+1)} \right]^n \quad (5.18)$$

and

$$\tilde{\bar{F}}^{(n)}(\tau) = \frac{1}{2(n!)} \left[\frac{\bar{a}}{\tau(\tau-1)} \right]^n \quad (5.19)$$

where

$$a = \frac{g^2}{32\pi^2} \ln \frac{q^2}{m^2} \quad (5.20)$$

and

$$\bar{a} = \frac{g^2}{32\pi^2} \ln \frac{q^2}{m^2} \quad (5.21)$$

Clearly Eq. (5.17) is satisfied and hence the reciprocal relation (4.7) follows.

Consider now the combination of analytic continuation and the reciprocal relation. Eliminating $\tilde{F}(\omega)$ between Eqs. (4.1) and (4.7) we have a condition on $F(\omega)$ itself,

$$F(\omega) = -\frac{1}{\omega} F\left(\frac{1}{\omega}\right). \quad (5.22)$$

We now state a theorem: If the transform $\tilde{F}(\tau)$ satisfies $\tilde{F}(\tau) = \tilde{F}(-\tau-1)$, and moreover if $\tilde{F}(\tau)$ has only isolated poles and/or essential singularities in τ then $F(\omega)$ satisfies Eq. (5.22). [By making the formal transition from Mellin transform to Laplace transform as in Eq. (5.3) and by shifting the origin in $\tilde{F}(\tau)$, $\tilde{G}(\tau) \equiv \tilde{F}(\tau - \frac{1}{2})$, then the statement of the theorem is changed as follows: Let $\tilde{G}(\tau)$ and $G(\tau)$ be Laplace transform pairs. Then if $\tilde{G}(\tau)$ is even(odd) in τ and moreover has only isolated poles and/or essential singularities in τ , then $G(z)$ is odd (even) in z .]

The proof is straightforward. First note that singularities of $\tilde{F}(\tau)$ come in pairs symmetrically located about the line $\text{Re}\tau = -1/2$. Suppose that $\tilde{F}(\tau)$ has a pole at $\tau=\alpha$ with residue γ . Because $\tilde{F}(\tau) = \tilde{F}(-\tau-1)$ we must also have a pole at $\tau=-(\alpha+1)$ with residue $-\gamma$. Use the inversion formula Eq. (5.2) and close the contour to the left picking up the singularities at $\tau=\alpha, -\alpha-1$ as illustrated in Fig. 15. One finds

$$F(\omega) = \gamma(\omega^\alpha - \omega^{-\alpha-1}) \quad (5.23)$$

which satisfies Eq. (5.22). The result may be immediately extended to a sum (finite or infinite) of simple pole singularities of $\tilde{F}(\tau)$. Since second order and higher poles can be build up from a coalescence of simple poles and an isolated essential singularity is just an infinite order pole the proof holds for such cases too. Hence the theorem is proven.

It is easy to see by taking as an example $\tilde{F}(\tau) = (\tau(\tau+1))^{-1/2}$ that the hypothesis of no branch points is necessary for the theorem. Likewise the hypothesis of isolated singularities was clearly used in our constructive proof.

The converse to this theorem is that given the relation (5.22) and some restriction on the class of functions $F(\omega)$ one must have $\tilde{F}(\tau) = \tilde{F}(-\tau-1)$. However, we are unable to give at this time a satisfactory characterization of the restriction except the too narrow one that $F(\omega)$ is the sum of terms of the form $\gamma\omega^\alpha$.

By inspection of Eq. (5.18), the result for the rainbow graphs in γ_5 theory, we see that the hypothesis of the theorem are satisfied, hence we may conclude that the self-reciprocal relation (5.22) is obeyed.

In the same spirit we state a final theorem which applies to the analytic continuation relation: If $\tilde{F}(\tau)$ and $\tilde{\tilde{F}}(\tau)$ have only isolated poles and essential singularities and satisfy $\tilde{F}(-\tau) = \tilde{\tilde{F}}(\tau)$ then the analytic continuation $\bar{F}(w) = -F(w)$ follows.

The proof is as above except that we also need the inversion formula for Eq. (5.16), which is

$$\bar{F}(w) = \int_{\bar{c} - i\infty}^{\bar{c} + i\infty} \frac{d\tau}{2\pi i} \bar{w}^{-\tau} \tilde{\tilde{F}}(\tau),$$

where the contour lies to the right of all singularities of $\tilde{\tilde{F}}(\tau)$.

Naturally the theorem is satisfied by the example given by Eqs. (5.18) and (5.19).

VI. CONSEQUENCES

In this final section we discuss further the reciprocal relation, Eq. (4.7), and some consequences which follow if it is taken seriously. This discussion is subject to the caveat that the reciprocal relation cannot be correct as it stands for all systems. In particular we can expect that the reciprocal relation does not apply to weakly bound composite systems like nuclei. By weakly bound we mean, of course, that the binding energy is small compared to the rest masses of the constituents.

One may ask about particles like the proton, pion, etc. We know that these particles also are composite systems. They are quite different from nuclei, however, since typical binding energies are of the same order of magnitude as the rest mass of constituents - whether one regards the hadrons as composites of themselves or of more elementary building blocks like quarks. While it is true that there is no compelling reason why the reciprocal relation, based as it is on perturbation theory, need apply to this latter class of tightly bound composite systems it will be amusing to see if it satisfied in some approximate way, nevertheless. Let us spell out a few consequences.

A. Multiplicity

One important experimental number is the average multiplicity of hadrons produced in annihilation. This quantity can be expressed as an integral over the inclusive cross-section. The result which we now show is that, when coupled with diffractive behavior in scattering, the reciprocal relation leads to logarithmic growth in multiplicity.

We imagine we scatter off nucleon targets and are measuring the inclusive annihilation experiment, cross section $d^3\bar{\sigma}/d^3p$, with detected nucleons, and that $F_L = \bar{F}_L = 0$. Then

$$\begin{aligned} \langle n \rangle &= \bar{\sigma}_T^{-1} \int d^3p \frac{d^3\bar{\sigma}}{d^3p} \\ &= \bar{\sigma}_T^{-1} \int d\omega d \cos \theta \frac{d^2\bar{\sigma}}{d\omega d\cos\theta}. \end{aligned} \quad (6.1)$$

We use Eq. (2.20), perform the $\cos \theta$ integral, make the one photon approximation $\bar{\sigma} = a_T/(q^2)$, and find

$$\langle n \rangle = \frac{8}{3} \pi \alpha^2 a_T^{-1} \int_{2\sqrt{m^2/q^2}}^{\omega} d\omega \bar{F}_T(\omega) \cdot \omega \quad (6.2)$$

$$= \frac{8}{3} \pi \alpha^2 a_T^{-1} \int_{2\sqrt{m^2/q^2}}^{\omega} d\omega F_T(1/\omega). \quad (6.3)$$

In going from (6.2) to (6.3) we have assumed the reciprocal relation (47). Now diffractive behavior in scattering means that $F_2 = \nu W_2 = C = \text{constant}$ for large ω , or

$$F_T(\omega) \xrightarrow{\omega \rightarrow \infty} \frac{1}{2} C \omega. \quad (6.4)$$

We see this behavior leads to a logarithmic divergence for small ω in (6.3),

$$\langle n \rangle = \frac{2}{3} \pi \alpha^2 a_T^{-1} C \ln \left[\frac{q^2}{m^2} \right] + \text{const.} \quad (6.5)$$

Such logarithmic growth is contrary to recent light cone arguments²⁵ which claim that $\bar{F}_T(\omega)$ is non-singular as $\omega \rightarrow 0$ and hence that $\langle n \rangle = \text{const.}$ This claim is contradicted in massive QED by the diffractive digrams as in Fig. 13(c), which give $\bar{F}_T(\omega) \rightarrow \omega^{-2}$, and in $\lambda\phi^3$ ²³, where $\bar{F}_T(\omega) \rightarrow \omega^{-1}$. Logarithmic growth in multiplicity due to the tower diagrams is a typical multiperipheral mechanism, and is different from the logarithmic growth

of mesons in Eq. (3.25).

B. Parton Model

It is natural to ask what is required to obtain the reciprocal relation in the parton model. One finds that it is necessary for $f(x)$, the probability of finding a parton constituent in a physical hadron having longitudinal momentum fraction $x(x=1/\omega)$, to be the same function as $g(\omega)$, where g is the probability of finding a physical hadron in a one parton state with fraction ω of the parton's longitudinal momentum. In general there is no need for the functions f and g to be so related.

However, in perturbation theory the physical hadrons are dressed partons (partons = bare quanta) and in the leading-logarithm approximation resemble the bare constituents closely enough that f and g are appropriately related.

In the parton model of Berman, Bjorken, and Kogut²⁶ the functions f and g , while not giving the reciprocal relation everywhere, are proportional in the reciprocal regions $x \rightarrow 0$, $\omega \rightarrow 0$ and therefore generate a logarithmic annihilation multiplicity like Eq. (6.5) given the diffractive inelastic behavior expressed by Eq. (6.4).

C. Dynamical Sum Rules

Given the reciprocal relation (4.7) and the existence of dynamical sum rules for inelastic scattering, e.g. the Adler Sum Rule²⁷, it is possible to write sum rules for the structure functions of annihilation. Recall the sum rules of inelastic scattering provide a unique test of the quantum numbers of the constituents of the hadrons. Given these quantum numbers, the reciprocal relation predicts easily

measured quantities like multiplicities in annihilation.

Unfortunately most of the inelastic scattering sum rules involve neutrino scattering, for which the annihilation counterpart is at present unrealistic. There is, however, one interesting sum rule for inelastic scattering which follows from combination of the Adler sum rule²⁷ and the exchange degeneracy relation²⁸,

$$\int_0^1 dx \left[F_1^{ep}(\omega) - F_1^{en}(\omega) \right] = \frac{1}{6}. \quad (6.6)$$

Application of Eq. (4.7) gives for annihilation

$$\int_0^1 d\omega \omega \left[\bar{F}_1^p(\omega) - \bar{F}_1^n(\omega) \right] = \frac{1}{6}. \quad (6.7)$$

With the help of Eq. (6.2) we can cast Eq. (6.7) into a prediction for the difference of proton and neutron multiplicities

$$\langle n_p \rangle - \langle n_n \rangle = \frac{1}{2}. \quad (6.8)$$

In obtaining Eq. (6.8) we have used in Eq. (6.2) the value $a_T = \frac{8}{9} \pi \alpha^2$. This value and the $\frac{1}{6}$ on the right hand sides of Eqs. (6.6) and (6.7) follow if the popular SU(3) quark model algebra applies. For an underlying SU(2) symmetry let $a_T = \frac{4}{3} \pi \alpha^2$ and change the right hand sides of Eqs. (6.6), (6.7) and (6.8) to $\frac{1}{2}$, $\frac{1}{2}$, and 1 respectively.

D. Kinematic Considerations

The physical region for annihilation, Eq. (2.12), is actually rather small (i.e. does not extend even approximately from 0 to 1) for most masses and presently available colliding ring energies. To take an example, even for $q^2 = 25(\text{Gev})^2$ and detected protons, ω runs only

from $\sim .4$ to $\sim .92$. The accessible region for pions in annihilation is much wider for a given q^2 ; we are already seeing evidence for copious pion production at present machine energies²⁹. If one wished to test the reciprocal relation for pions one would require deep inelastic scattering from pions. The possibility of accumulating this data, using a region in which one-pion exchange is visible in scattering from nucleons, has recently been discussed³⁰.

VII. Summary

In this paper we have studied the annihilation process $e^- + e^+ \rightarrow \bar{P} + X$ in the neutral-vector-gluon model in the Bjorken limit. We find, using a leading-logarithm approximation, results which closely resemble the inelastic scattering channel $e^- + P \rightarrow e^- + X$. Namely, for each definite final state, Bjorken scaling is broken by $\ln^2 q^2$ factors which exponentiate into an eikonal-like form after summation over final states. There is also a close interplay between virtual meson form factor corrections and the emitted mesons. Copious "soft" vector meson emission characterizes the final states. In particular the multiplicity grows like $\ln^2 q^2$.

We also find, after taking cognizance of the branch points in q^2 which are present because of the scale breaking $\ln q^2$ factors, that the annihilation structure functions can be reached by analytic continuation of the inelastic scattering structure functions.

Finally we observe and study a reciprocal relation which connects the annihilation and inelastic structure functions in their respective physical regions. This study is facilitated by use of the longitudinal impact parameter representation. We show here that this representation is a natural extension of the ordinary Regge representation cum Bjorken scaling.

Appendix A

This Appendix contains details behind the results for the low order diagrams which we quoted in Sec. III. We use the notation and Lorentz frame discussed there, and refer to the figures for the momentum labels.

A. Diagram 8(a)

$$\bar{F}_1^{8(a)} = \frac{\lambda}{4\pi} \int \frac{du' du_1}{u' u_1} \int d^2P' d^2k_1 \delta^+(\omega^{-1} - 1 - u_1 - u') \times \delta^\perp(\vec{P}' + \vec{k}_1) \delta^-(q^2 \omega - m^2 - P'^2 - k_1^2) \frac{N}{D} \quad (\text{A.1})$$

where

$$N \doteq \text{Tr} \left\{ \gamma_\alpha \not{P}' \gamma^\alpha (\not{P}' + \not{k}_1) \gamma^1 \not{P}' \gamma^1 (\not{P}' + \not{k}_1) \right\} \quad (\text{A.2})$$

and

$$D = [(P+k_1)^2 - m^2]^2 = (\vec{k}_1^2 + A_1)^2 u_1^{-2}, \quad (\text{A.3.})$$

$$A_1 = u^2(1+u_1) + m^2 u_1^2 > 0$$

In writing Eq. (A.2) we have dropped fermion mass terms; they make no contribution to the leading logarithmic answer. [Throughout this section +, \perp , - superscripts on delta functions are used for a convenient reminder that these delta functions express conservation of +, \perp , - momentum respectively.]

Without loss of generality we take \vec{P}' to be in the 2-direction, and find

$$N \doteq 16 P \cdot k_1 P'^2 k_1^2. \quad (\text{A.2'})$$

We next perform the \vec{P}' and u' integrations by means of δ^\perp and δ^- respectively. For the \vec{k}_1 integration there are two regions to be considered:

If \vec{k}_1^2 is comparable to q^2 , then $N \propto (\vec{k}_1^2)^2$ and the integration is not logarithmic. If $\mu^2 \ll \vec{k}_1^2 \ll q^2 \omega u_1$, then $N \propto \vec{k}_1^2$ and the integration is logarithmic. The latter obviously gives the leading behavior. Therefore

$$N \doteq 4k_1^- u_1 P^+ \doteq 4 \vec{k}_1^2 q^2 \omega \quad (\text{A.2'').})$$

and

$$\bar{F}_1^{8(a)} \doteq \lambda \int du_1 u_1 \int_{\frac{\mu^2}{\epsilon}}^{\epsilon q^2 \omega u_1} d(\vec{k}_1^2) \frac{\vec{k}_1^2 \delta^+ (\omega^{-1} - 1 - u_1 - \frac{\vec{k}_1^2}{q^2 \omega})}{[\vec{k}_1^2 + A_1]^2} \quad (\text{A.4})$$

$$\doteq \lambda \int du_1 u_1 \ln \left(\frac{q^2}{\mu^2} \right) \delta^+ (1 + u_1 - \omega^{-1}). \quad (\text{A.5.})$$

Thus we find a result which is proportional to a single logarithm. Moreover we note that the u_1 integration is such that the integral of \bar{F}_1 over ω cannot generate an additional logarithm. It is for this reason we have dropped the ωu_1 factor in the argument of the logarithm in going from Eq. (A4) to Eq. (A5).

B. Diagram 8(c)

The expression for $\bar{F}_1^{8(c)}$ is given by Eq. (A1) with

$$N \doteq \text{Tr} \left\{ \not{P} \gamma^1 (\not{P} + \not{k}_1) \gamma^\alpha (\not{P}') \gamma^1 (\not{P} + \not{k}_1) \gamma_\alpha \right\} \quad (\text{A.6.})$$

and

$$D = [(\not{P} + \not{k}_1)^2 - m^2][(\not{P}' + \not{k}_1)^2 - m^2] \\ \doteq u_1^{-1} [\vec{k}_1^2 + A_1] [(\omega^{-1} - 1) q^2 \omega - \vec{k}_1^2]. \quad (\text{A.7.})$$

Again with \vec{P}' in the 2-direction, we have

$$N \doteq 16 \not{P} \cdot \not{P}' (\not{P} + \not{k}_1) \cdot (\not{P}' + \not{k}_1). \quad (\text{A.6'}.)$$

We do the \vec{P}' and u' integrals with δ^+ and δ^- . The \vec{k}_1^2 integration is logarithmic only in the interval $\mu^2 \ll \vec{k}_1^2 \ll q^2 \omega u_1$. Knowing this we can make the approximations

$$P \cdot P' \approx q^2 \omega, \quad (P+k_1) \cdot (P'+k_1) \approx (1+u_1) q^2 \omega \quad (\text{A.8.})$$

so that

$$N \doteq 4(q^2 \omega)^2 (1+u_1) \quad (\text{A.6'.})$$

and

$$D \doteq u_1^{-1} (\vec{k}_1^2 + A_1) (1-\omega) q^2.$$

Therefore

$$\begin{aligned} \bar{F}_1^{8(c)} &\doteq \lambda \int \frac{du_1}{u_1} \int_{\frac{\mu^2}{\varepsilon}}^{\varepsilon q^2 \omega u_1} d(\vec{k}_1^2) \frac{\omega(1+u_1)u_1}{(1-\omega)(\vec{k}_1^2 + A_1)} \delta^+(\omega^{-1} - 1 - u_1 - \frac{\vec{k}_1^2}{q^2 \omega}) \\ &\doteq \lambda \frac{\omega}{(1-\omega)} \int du_1 (1+u_1) \delta^+(\omega^{-1} - 1 - u_1) \ln \left(\frac{q^2 \omega u_1}{\mu^2} \right). \quad (\text{A.9.}) \end{aligned}$$

The remaining integral over u_1 is done by the δ^+ function. The result has a single overall power of $\ln q^2$. Because of the overall $(1-\omega)^{-1}$ overall factor a second logarithmic power can be generated if we integrate over ω in the region $\omega \approx 1$. This time, therefore, we are careful to retain the u_1 term in the argument of the logarithm in Eq. (A.9.). Thus we have the result quoted in Eq. (3.11).

C. Diagrams 9(a) and 9(b)

Although it is instructive to consider these diagrams separately, it is most efficient to combine the calculations as we shall do here. We have

$$\bar{F}_1^{g(a), g(b)} = \frac{\lambda^2}{4\pi^2} \int \frac{du_1 du_2 du'}{u_1 u_2 u'} \int d^2 k_1 d^2 k_2 d^2 P' \times \delta^+(\omega^{-1} - 1 - u_1 - u_2 - u') \delta^1(\vec{P}' + \vec{k}_1 + \vec{k}_2) \delta^-(q^2 \omega - P'^- - k_1^- - k_2^-) \frac{N^{(a), (b)}}{D^{(a), (b)}} \quad (\text{A.10.})$$

where

$$N^{(a)} \doteq \text{Tr} \left\{ (\not{P} + \not{k}_1 + \not{k}_2) \gamma_\alpha (\not{P} + \not{k}_1) \gamma_\beta \not{P}' \gamma^1 (\not{P}' + \not{k}_1 + \not{k}_2) \gamma^\beta (\not{P}' + \not{k}_2) \gamma^\alpha \not{P}' \gamma^1 \right\}, \quad (\text{A.11.})$$

$$D^{(a)} = [(P + k_1)^2 - m^2] [(P + k_1 + k_2)^2 - m^2] [(q - P)^2 - m^2] [(q - P - k_1)^2 - m^2], \quad (\text{A.12})$$

$$N^{(b)} \doteq \text{Tr} \left\{ (\not{P} + \not{k}_1 + \not{k}_2) \gamma_\alpha (\not{P} + \not{k}_2) \gamma_\beta \not{P}' \gamma^1 (\not{P}' + \not{k}_1 - \not{k}_2) \gamma^\alpha (\not{P}' + \not{k}_2) \gamma^\beta \not{P}' \gamma^1 \right\}, \quad (\text{A.13.})$$

and

$$D^{(b)} = [(P + k_2)^2 - m^2] [(P + k_1 + k_2)^2 - m^2] [(q - P)^2 - m^2] [(q - P - k_1)^2 - m^2]. \quad (\text{A.14.})$$

We may now apply the lessons learned from the lower order diagrams.

To extract the leading behavior of the numerators let the - momentum introduced by q flow along the P' line and the + momentum flow along the P line. One finds

$$N^{(a)} \doteq 8(1 + u_1 + u_2) (1 + u_1) P'^- (P'^- + k_2^-) (P'^- + k_1^- + k_2^-). \quad (\text{A.11'.})$$

After identifying the region over which the \vec{k}_i integrations are logarithmic one has $P'^- \approx q^2 \omega \gg k_i^-$ so that (A.11'.) may be further simplified to

$$N^{(a)} \doteq 8(1+u_1+u_2) (1+u_1) (q^2\omega)^3. \quad (\text{A.15.})$$

Similarly we can simplify Eq. (A.13.) to

$$N^{(b)} \doteq 8(1+u_1+u_2) (1+u_2) (q^2\omega)^3. \quad (\text{A.16.})$$

In the same fashion we exploit the fact that in the important integration regions $q^- \gg k_1^-$, P^- in order to simplify the last two factors of $D^{(a),(b)}$ according to

$$[(q-P)^2-m^2] [(q-P-k_1)^2-m^2] \doteq [(1-\omega)q^2] [(\omega^{-1}-1-u_1)q^2\omega]. \quad (\text{A.17.})$$

At this point we combine the two integrands. We have a situation analogous to Eq. (3.8) of I, in which the sum of two diagrams can be drastically simplified. The analogous simplification here goes as follows:

$$\begin{aligned} \frac{N}{D} &\doteq \frac{N^{(a)}}{D^{(a)}} + \frac{N^{(b)}}{D^{(b)}} = \frac{8(1+u_1+u_2)(q^2\omega^2)}{(1-\omega)(\omega^{-1}-1-u_1)} \\ &\times \left\{ \frac{1}{(P+k_1+k_2)^2-m^2} \left[\frac{1+u_1}{(P+k_1)^2-m^2} + \frac{1+u_2}{(P+k_2)^2-m^2} \right] \right\} \\ &\doteq \frac{8(1+u_1+u_2)q^2\omega^2}{(1-\omega)(\omega^{-1}-1-u_1)} \left\{ \frac{1}{[(P+k_1)^2-m^2][(P+k_2)^2-m^2]} \right\}. \quad (\text{A.18.}) \end{aligned}$$

We see that the net result as far as the \vec{k}_1 and \vec{k}_2 integrations are concerned is a factorization into two pieces, each identical in form to the transverse integration for diagram 8(c).

One completes the calculation as follows: First perform the \vec{P}' and u' integrations using δ^+ and δ^- respectively. Noting that

$$[(P+k_i)^2 - m^2] = u_i^{-1} (\vec{k}_i^2 + A_i) \quad (\text{A.19.})$$

one obtains

$$\begin{aligned} \bar{F}_1^{g(a)+g(b)} &\doteq 2\lambda^2 \int \frac{du_1 du_2}{(1-\omega)(\omega^{-1}-1-u_1)} \int \frac{d^2k_1}{\pi} \frac{1}{(\vec{k}_1^2 + A_1)} \\ &\times \int \frac{d^2k_2}{\pi} \frac{1}{(\vec{k}_2^2 + A_2)} \delta^+(\omega^{-1}-1-u_1-u_2-0(\frac{\vec{k}_i^2}{q^2})). \end{aligned} \quad (\text{A.20.})$$

The leading logarithms come from $\mu^2 \ll \vec{k}_i^2 \ll q^2 \omega u_i$; we call these ultra-violet logarithms. Because of the limits on the \vec{k}_i , the δ^+ argument simplifies to $\delta^+(\omega^{-1}-1-u_1-u_2)$. The remaining longitudinal integrations are strongly coupled. In particular the denominator factor $(\omega^{-1}-1-u_1) = u_2$ shows the u_2 integration is logarithmic over the interval $\mu^2/(\epsilon q^2) < u_2 < \epsilon u_1$; we call this an infrared logarithm. The final u_1 integral is performed with the aid of the δ^+ function, which by now takes the form $\delta^+(\omega^{-1}-1-u_1)$. The final result is given in Eq. (3.12).

Appendix B

In this Appendix we verify the analytic continuation formula Eq. (4.1) and the reciprocal relation, Eq. (4.7), for the lowest order "diffractive" diagrams illustrated in Figs. 13(a) and 13(b). These figures are drawn for the scattering case; their annihilation analogs are obvious.

For Fig. 13(a) we have (recall $-q^2 \equiv Q^2 > 0$)

$$F_1^{13(a)} \doteq \frac{1}{\pi^2} \left(\frac{-g^2}{32\pi^2} \right)^2 \int \frac{dx_1 dx_2 dx'}{x_1 x_2 x'} \int d^2 \ell_1 d^2 \ell_2 d^2 p' \times \delta^+(1-\omega^{-1}-x'-x_1-x_2) \delta^+(\vec{p}' + \vec{\ell}_1 + \vec{\ell}_2) \delta^-(\omega Q^2 - \frac{\vec{p}'^2}{x'} - \frac{\vec{\ell}_1^2}{x_1} - \frac{\vec{\ell}_2^2}{x_2}) \frac{N}{D} \quad (\text{B.1.})$$

where

$$p' = (x', \vec{p}', \frac{\vec{p}'^2 + m^2}{x'})$$

$$\ell_i = (x_i, \vec{\ell}_i, \frac{\vec{\ell}_i^2 + \mu^2}{x_i})$$

and

$$N \doteq \text{Tr} \left\{ \not{p} \gamma_5 \not{p}' \gamma_5 \right\} \text{Tr} \left\{ \not{k}_2 \gamma^1 (\not{p}' - \not{p} + \not{\ell}_1) \gamma_5 \not{\ell}_1 \gamma_5 (\not{p}' - \not{p} + \not{\ell}_1) \gamma^1 \right\}$$

$$\doteq 32 p \cdot p' [\ell_2 \cdot (p' - p) \ell_1 \cdot (p' - p) + \ell_1 \cdot \ell_2 p \cdot p'] \quad (\text{B.2.})$$

$$D = [(p' - p)^2 - \mu^2]^2 [(p' - p + \ell_1)^2 - m^2]^2$$

$$\doteq (2 p \cdot p')^2 (-2 p \cdot p' - 2 p \cdot \ell_1 + 2 p' \cdot \ell_1)^2. \quad (\text{B.3.})$$

The factor N/D in Eq. (B.1.) is the function f_3 we discussed in part C of Sec. IV. We want to simplify f_3 keeping only those pieces which make maximal logarithmic contributions.

Rather than doing a rigorous mathematical exploration of all the regions over which f is integrated, we present here an analysis based on the physics of momentum flow. This analysis is supported by a more careful study. The large minus momentum introduced by q will be proportioned between k_1 and k_2 in all possible ways. However, no more than an ϵ fraction of q^- can leak through the meson line $p'-p$ and end up on the fermion line p' . This follows because any larger leakage will make the meson propagator large and hence suppress the result. We conclude therefore that no component of p' is large. Therefore since $q^- = O(Q^2)$ we can anticipate

$$\ell_1 \cdot \ell_2, p \cdot \ell_1, p \cdot \ell_2, p' \cdot \ell_1, p' \cdot \ell_2 = O(Q^2) \quad (\text{B.4.})$$

and

$$p' \cdot p = O(1). \quad (\text{B.5.})$$

Therefore

$$\begin{aligned} f_3(p \cdot p', p \cdot \ell_1, p \cdot \ell_2; \ell_1 \cdot \ell_2) &\equiv \frac{N}{D} \\ &\doteq \frac{8(p \cdot p') \ell_2 \cdot (p' - p) \ell_1 \cdot (p' - p)}{(p \cdot p')^2 [2\ell_1 \cdot (p' - p)]^2} \doteq \frac{2\ell_2 \cdot (p' - p)}{(p \cdot p') \ell_1 \cdot (p' - p)} \\ &\doteq \frac{2}{p \cdot p'} \left(\frac{\ell_2^-}{\ell_1^-} \right) \doteq \frac{4}{\left(\frac{p_1'^2}{x_1'} \right)} \frac{\left(\frac{x_2^2}{x_1^2} \right)}{\left(\frac{x_1^2}{x_1} \right)}. \end{aligned} \quad (\text{B.6.})$$

For the annihilation diagram analog we have

$$\bar{F}_1^{13(a)} \doteq \frac{1}{\pi^2} \left(\frac{g}{32\pi^2} \right)^2 \frac{du_1 du_2 du'}{u_1 u_2 u'} d^2 k_1 d^2 k_2 d^2 p'$$

$$\begin{aligned}
& \chi \delta^+ (\omega^{-1} - 1 - u' - u_1 - u_2) \delta^+ (\vec{p} + \vec{k}_1 + \vec{k}_2) \delta^- (q^2 \omega - \frac{\vec{p}^2}{u'} - \frac{\vec{k}_1^2}{x_1} - \frac{\vec{k}_2^2}{x_2}) \\
& \chi f_3(-P \cdot P', -P \cdot k_1, -P \cdot k_2; k_1 \cdot k_2) \quad (B.7.)
\end{aligned}$$

Again after a simple consideration of momentum flow

$$\begin{aligned}
f_3(-P \cdot P', -P \cdot k_1, -P \cdot k_2; k_1 \cdot k_2) & \doteq \frac{2}{P \cdot P'} \left(\frac{k_2^-}{k_1^-} \right) \\
& \doteq \frac{4}{\left(\frac{\vec{p}^2}{u_1} \right)} \cdot \left(\frac{\frac{\vec{k}_2^2}{u_2}}{\frac{\vec{k}_1^2}{u_1}} \right) \quad (B.8.)
\end{aligned}$$

To establish analytic continuation one need only make in Eqs. (B.1.) and (B.6.) the variable changes $x_i \rightarrow -u_i$, $\vec{\lambda}_i \rightarrow \vec{k}_i$, $x' \rightarrow -u'$, $\vec{p}' \rightarrow \vec{P}'$.

To establish the reciprocal relation we perform the scalings given in Eq. (4.18). One finds

$$\frac{2}{p \cdot p'} \frac{\lambda_2^-}{\lambda_1^-} \rightarrow \omega^2 \frac{2}{P \cdot P'} \frac{k_2^-}{k_1^-} \quad (B.9.)$$

which agrees with Eq. (4.19) since $N=3$. This completes the proof.

If one actually carries out the momentum integrations in Eq. (B.1.) after having approximated the integrand according to Eq. (B.6.) one finds the following. One finds two (nested) ultraviolet logarithms coming from the λ_1 and λ_2 transverse integrations. The longitudinal integrations are not logarithmic. Thus the diagram is $O(g^4 \ln^2 Q^2)$ with no special enhancements in ω . This graph is therefore of the same size and importance as the $O(g^4)$ outer rainbow (ladder) diagram.

The other $O(g^4)$ diffractive diagram is shown in Fig. 9(b). A similar analysis shows that this graph contains only a single power of $\ln Q^2$. Both the analytic continuation and reciprocal relation can be established by the same techniques as we have used for diagram 13(a).

Acknowledgments

We would like to thank A. I. Sanda for conversations on discontinuities of the Compton amplitude. Further thanks are due to J. D. Bjorken, J. C. Polkinghorne, and A. suri for discussions on various topics covered here.

References

1. P.M. Fishbane and J.D. Sullivan, Physics Letters 37B, 68 (1971); Phys. Rev. D4 2516 (1971), hereafter known as I.
2. P.M. Fishbane and J.D. Sullivan, Phys. Rev. D (to be published), hereafter known as II.
3. P.M. Fishbane and J.D. Sullivan, Phys. Rev. D4, 458 (1971).
4. J.D. Bjorken, Phys. Rev. 179, 1547 (1969).
5. S.J. Chang and P.M. Fishbane, Phys. Rev. D2, 1173 (1970).
6. S.D. Drell, D.J. Levy, and T.M. Yan, Phys. Rev. 187, 2159 (1969); Phys. Rev. D1, 1617 (1970).
7. P.V. Landshoff and J.C. Polkinghorne, DAMTP report #72/16; J. Pestieau and P. Roy, Phys. Letters 30B, 483 (1969); P.V. Landshoff, J.C. Polkinghorne, and R.D. Short, Nucl. Phys. B28, 225 (1971); R. Gatto and P. Menotti, Nuovo Cimento 7A, 118 (1972); J. Layssac and F.M. Renard, Nuovo Cimento 6A, 134 (1971); J.W. Moffat and V.G. Snell, Phys. Rev. D4, 1452 (1971).
8. These questions have been explored by V.N. Gribov and L.N. Lipatov, Phys. Lett. 37B, 78 (1971); Yad. Physica (to be published).
9. S.L. Adler and W.K. Tung, Phys. Rev. Letters 22, 978 (1969); R. Jackiw and G. Preparata, ibid 22, 975 (1969).
10. S.J. Chang and P.M. Fishbane, Phys. Rev. D2, 1084 (1970); T.K. Gaisser and J.C. Polkinghorne, Nuovo Cimento 1A, 501 (1971); A. Mason, J. Math. Phys. (to be published).
11. G. Altarelli and H.R. Rubinstein, Phys. Rev. 187, 2111 (1969); T.K. Gaisser and J.C. Polkinghorne, ref. 10; and ref. 6.

12. This represents a failure of the "contiguous vertex approximation", J.C. Polkinghorne, Nuovo Cimento 8A, 592 (1972). R. Jackiw and R.E. Waltz, MIT Report 266, have used formal field theory methods to study this point. See also T.M. Yan, Cornell Reports 184, 185
13. See also ref. 5 and the first paper of ref. 10, which together contain the relation.
14. This subject is treated at length in A. suri, Phys. Rev. D4, 570 (1971).
15. We use invariant normalization such that for bosons the density is $(2k_0)^{-1}$ per unit volume and for fermions the density is (m/E) .
16. For convenience in comparison we average over the antiproton spin in annihilation; experimentally one sums.
17. J.D. Sullivan, Nuclear Phys. B22, 358 (1970); J.D. Sullivan and W.T. Potter, Nuovo Cimento 3A, 93 (1971); A. suri, ref. 14.
18. P.V. Landshoff and J.C. Polkinghorne, ref. 7.
19. This quantity is twice the fraction of total center-of-mass energy $\sqrt{q^2}$ taken by the detected hadron.
20. C.G. Callan and D.J. Gross, Phys. Rev. Letters 22, 156 (1969).
21. Since the origin of the $(\omega-1)^{-1}$ factor is an s-channel pole, it remains unchanged save for the (apparent) sign.
22. See the third and fourth entries of ref. 7, and Gaisser and Polkinghorne, ref. 10.
23. R.L. Jaffe and H.C.L. Smith, unpublished.
24. H.D.I. Abarbanel, M.L. Goldberger, and S.B. Treiman, Phys. Rev. Letters 22, 500 (1969).

25. C.G. Callan and D.J. Gross, Princeton U. report.
26. S.M. Berman, J.D. Bjorken, and J.B. Kogut, Phys. Rev. D4, 3388 (1971).
27. S.L. Adler, Phys. Rev. 143, 1144 (1966).
28. P.M. Fishbane and D.Z. Freedman, Phys. Rev. (to be published).
29. C. Bernardini, in Proceedings, 1971 International Symposium on Electron and Photon Interactions at High Energies, Cornell University, Ithaca, New York., p. 38, (1972).
30. J.D. Sullivan, Phys. Rev. D5, 1732 (1972).

Figure Captions

1. Three physical processes considered in the text. (a) inelastic scattering, (b) three-body annihilation, (c) ordinary annihilation.
2. The physical regions for the three processes illustrated in Fig. 1.
3. The Compton amplitude. Various discontinuities of this amplitude control the physical processes of Fig. 1.
4. The discontinuities of the Compton amplitude which give the physical processes (a) - (c) respectively in Fig. 1.
5. The positions of the cuts for the physical processes in Fig. 1. and the paths which must be followed in taking the discontinuities in Fig. 4.
6. The physical regions for the processes similar to those in Fig. 1, but with proton, antiproton interchange.
7. Born diagram for annihilation. The heavy line indicates the detected particle.
8. $O(e^2)$ graphs for annihilation in massive QED. (a) and (b) are the analogues to the "outer" and "inner rainbows" of inelastic scattering, while (c), which gives a leading contribution, as explained in the text, is the "inner-outer rainbow" analogue. The heavy line indicates the detected particle.
9. Two-meson intermediate state inner-outer graphs. To leading-logarithmic accuracy, these two graphs combine in an eikonal-like fashion.
10. The general leading graph without form factor corrections. The shaded areas imply that a sum over all orders of connection of the vector meson legs is taken.

11. The general leading graph including the leading form factor corrections. The shaded areas again indicate a sum over all permutations of meson emission and absorption.
12. Lowest order outer rainbow, or ladder, diagram for inelastic scattering in massive QED.
13. Lowest order diffractive graphs. (a) and (b) are in γ_5 theory and (c) and (d) are in massive QED. Diagram (a) is more important than diagram (b) by a power of $\ln q^2$. In the same way (c) dominates (d) (Feynman gauge).
14. The general graph for inelastic scattering which expresses the contiguous vertex approximation. The interacting particle is point-like.
15. Contours in the τ -plane. C_i is the initial contour. C_f is the final contour, which encloses the contributions of poles and isolated essential singularities lying symmetrically about the point $\text{Re } \tau = -1/2$.

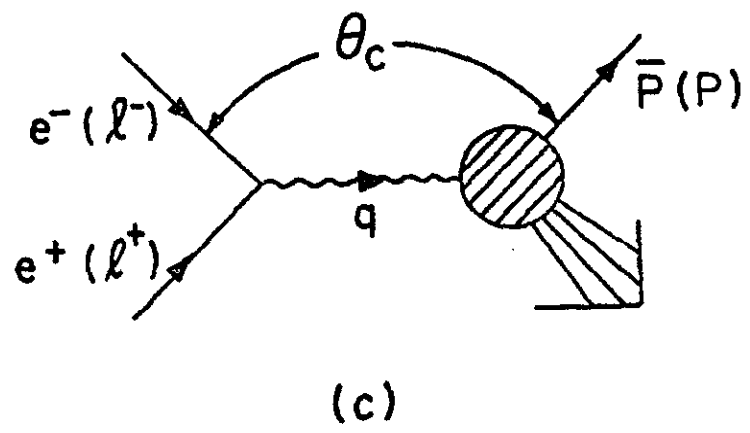
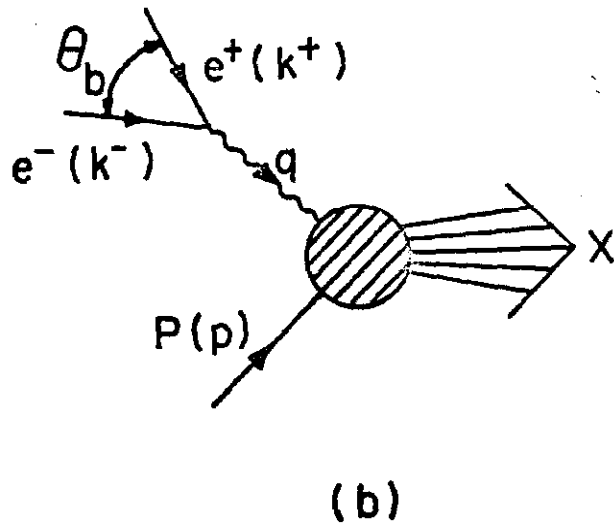
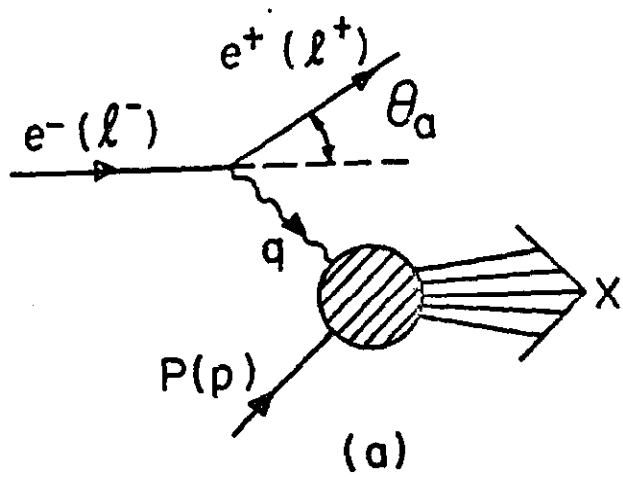


Figure 1

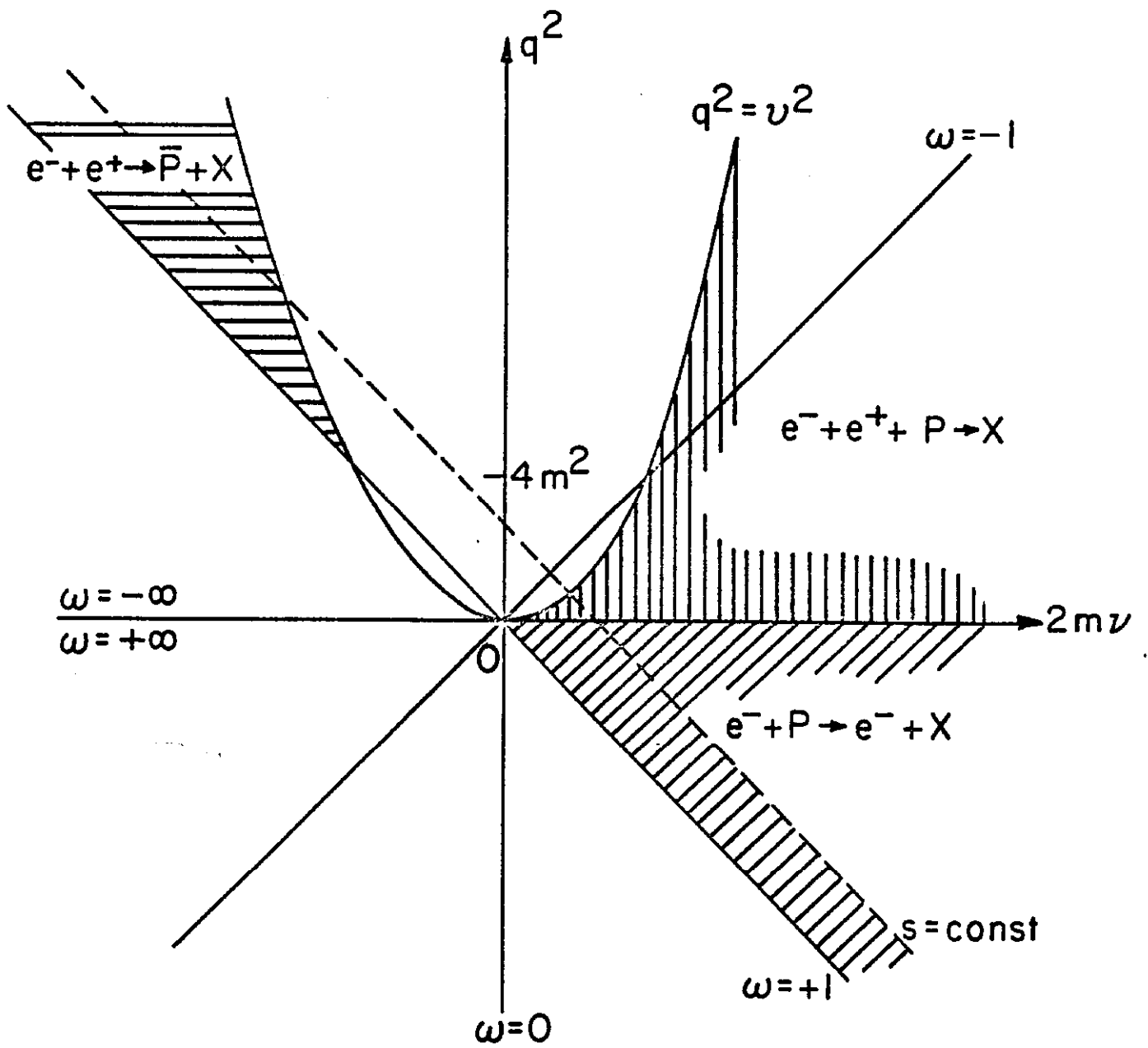


Figure 2

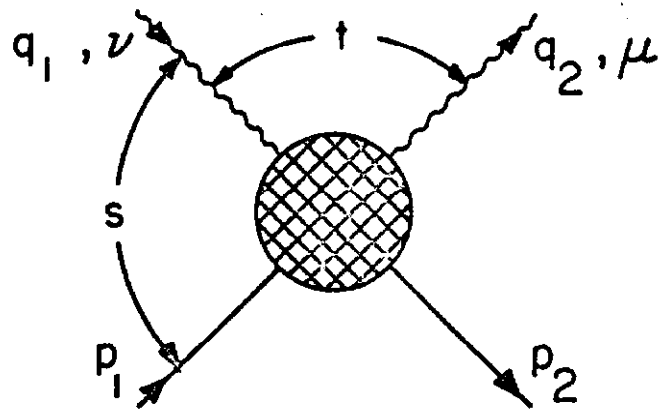
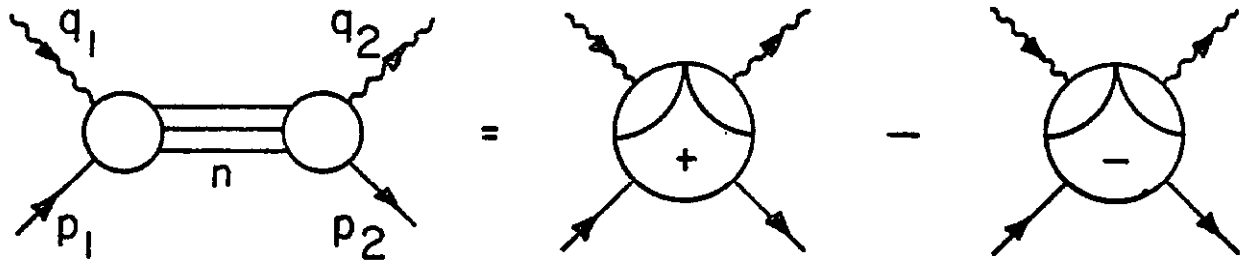
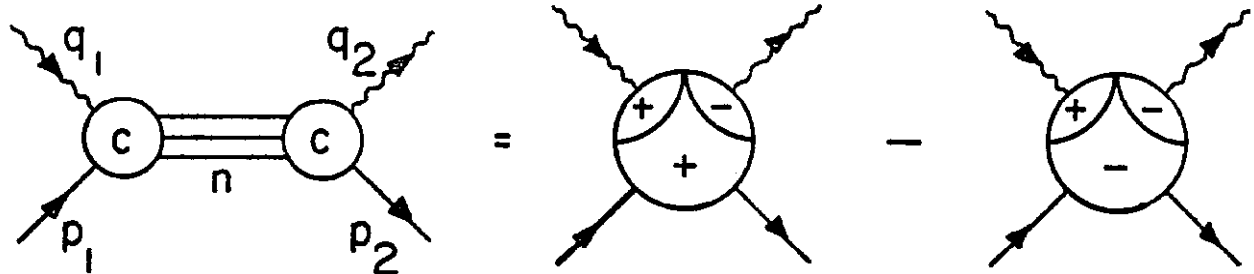


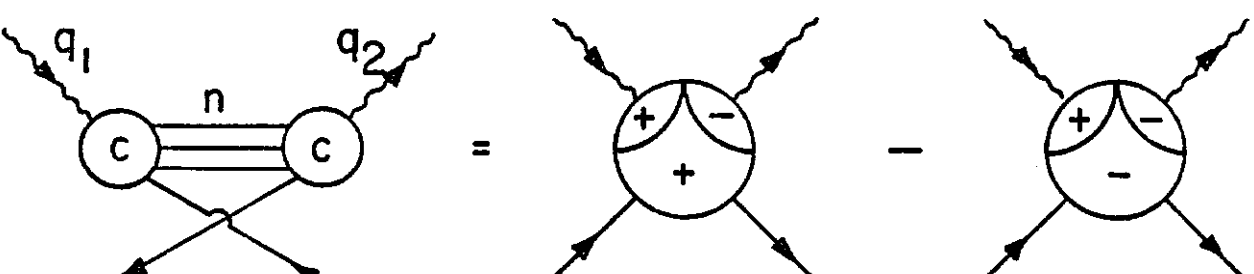
Figure 3



(a)



(b)



(c)

Figure 4

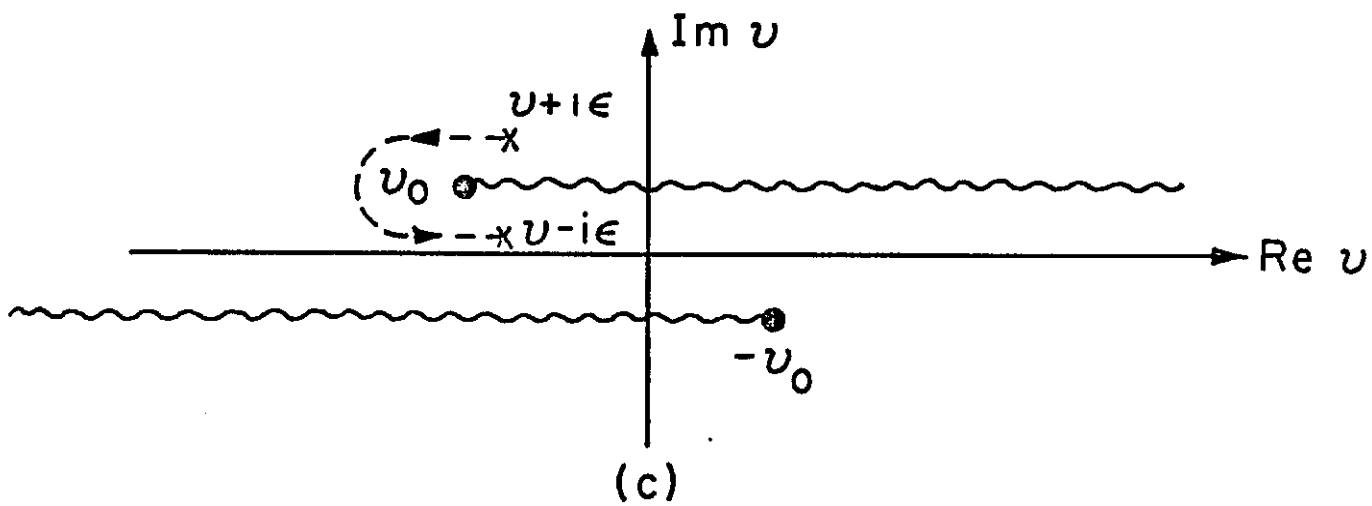
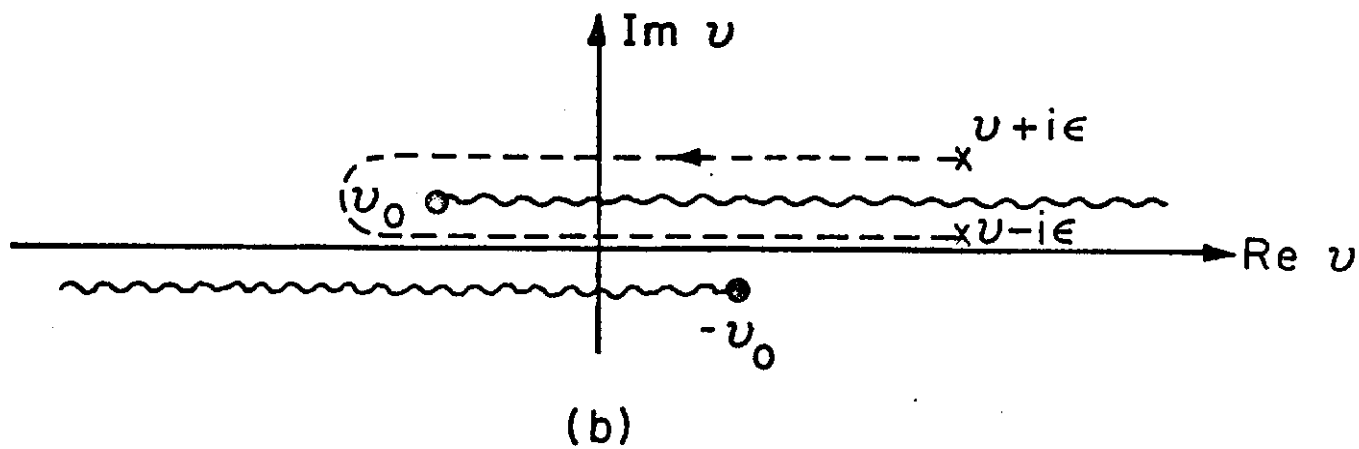
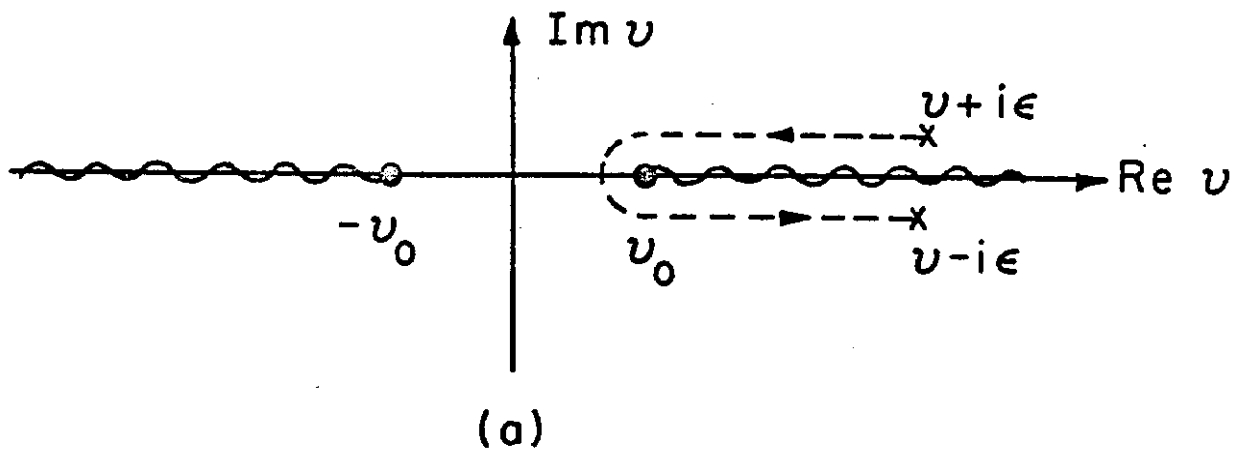


Figure 5

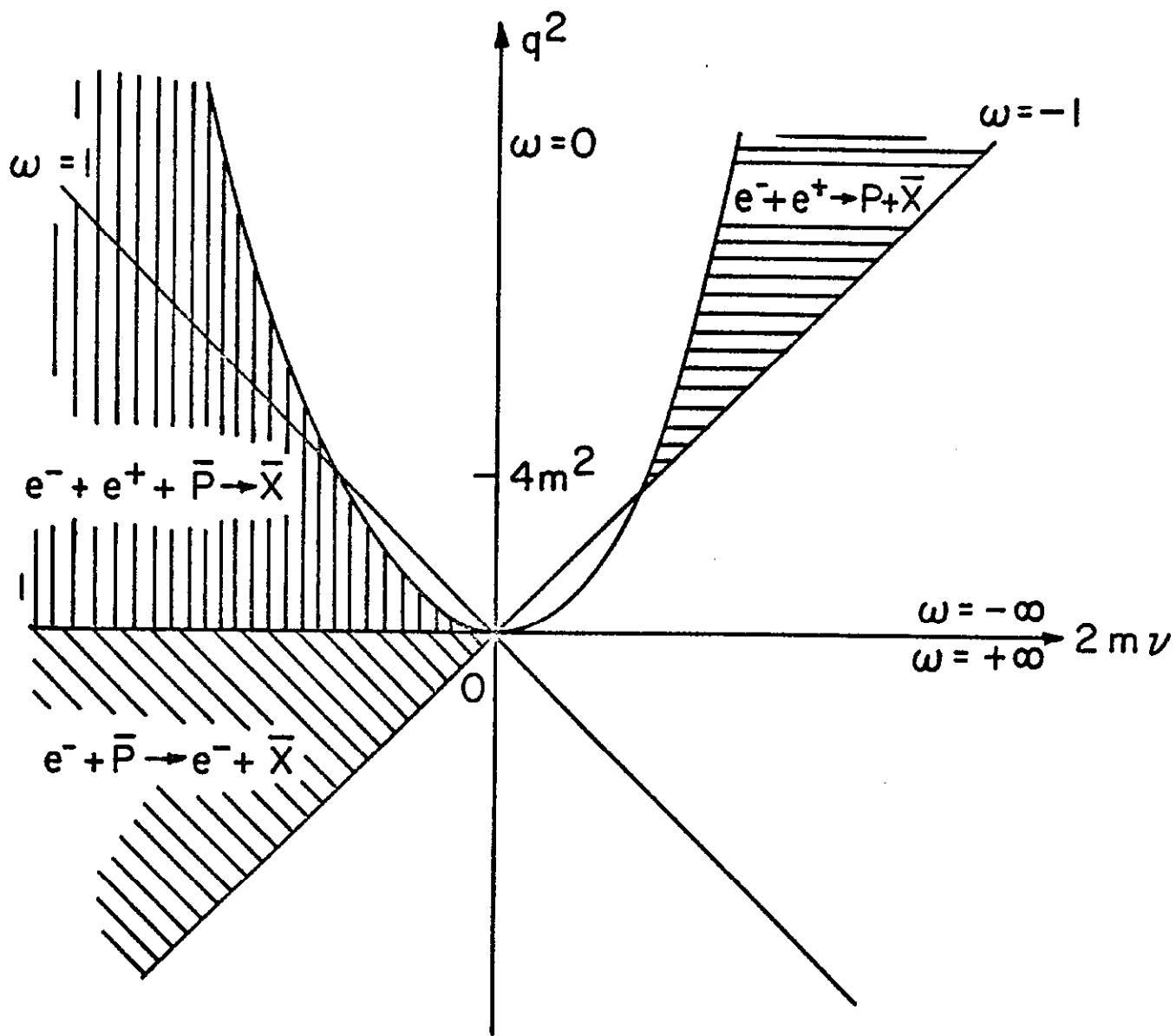


Figure 6

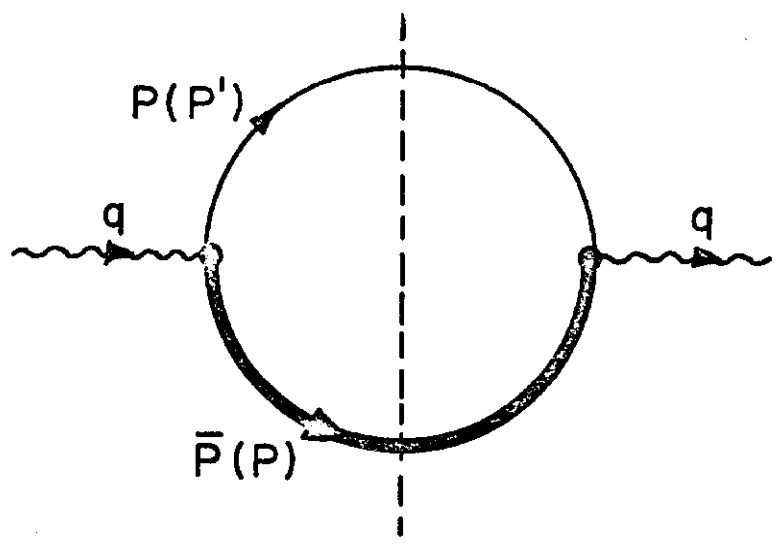


Figure 7

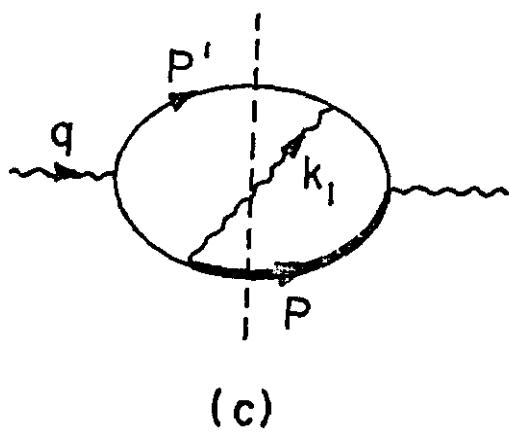
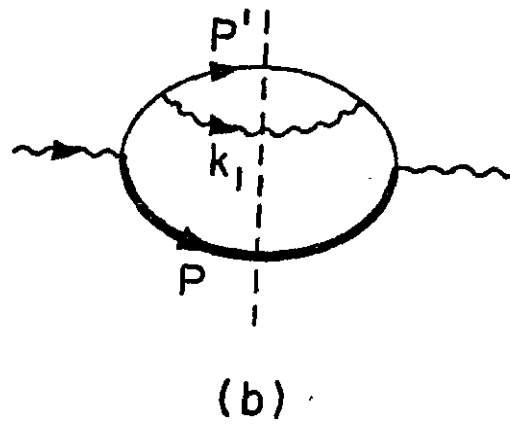
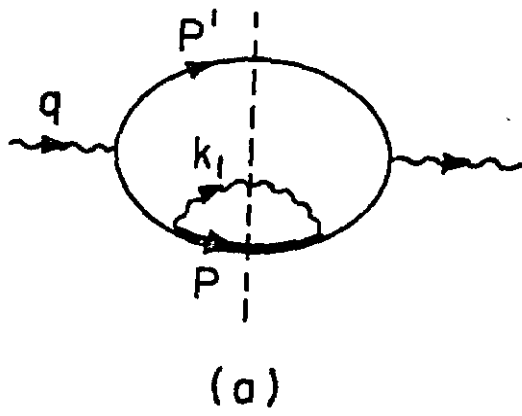


Figure 8

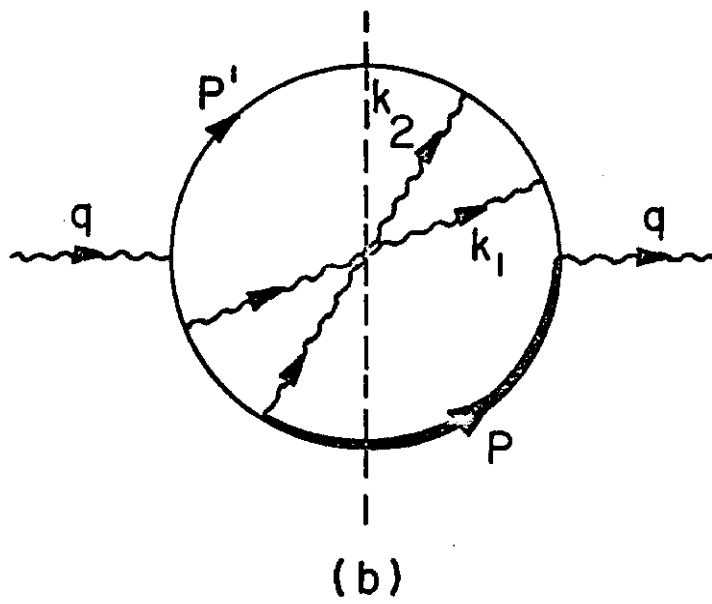
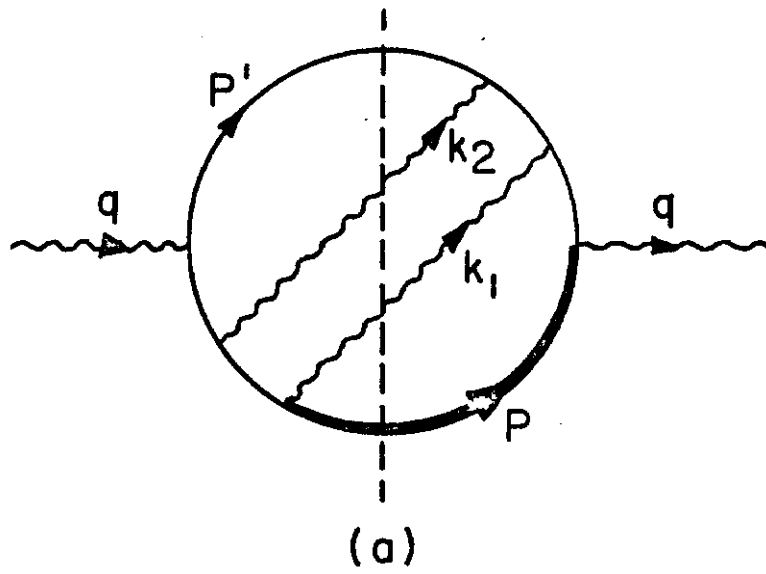


Figure 9

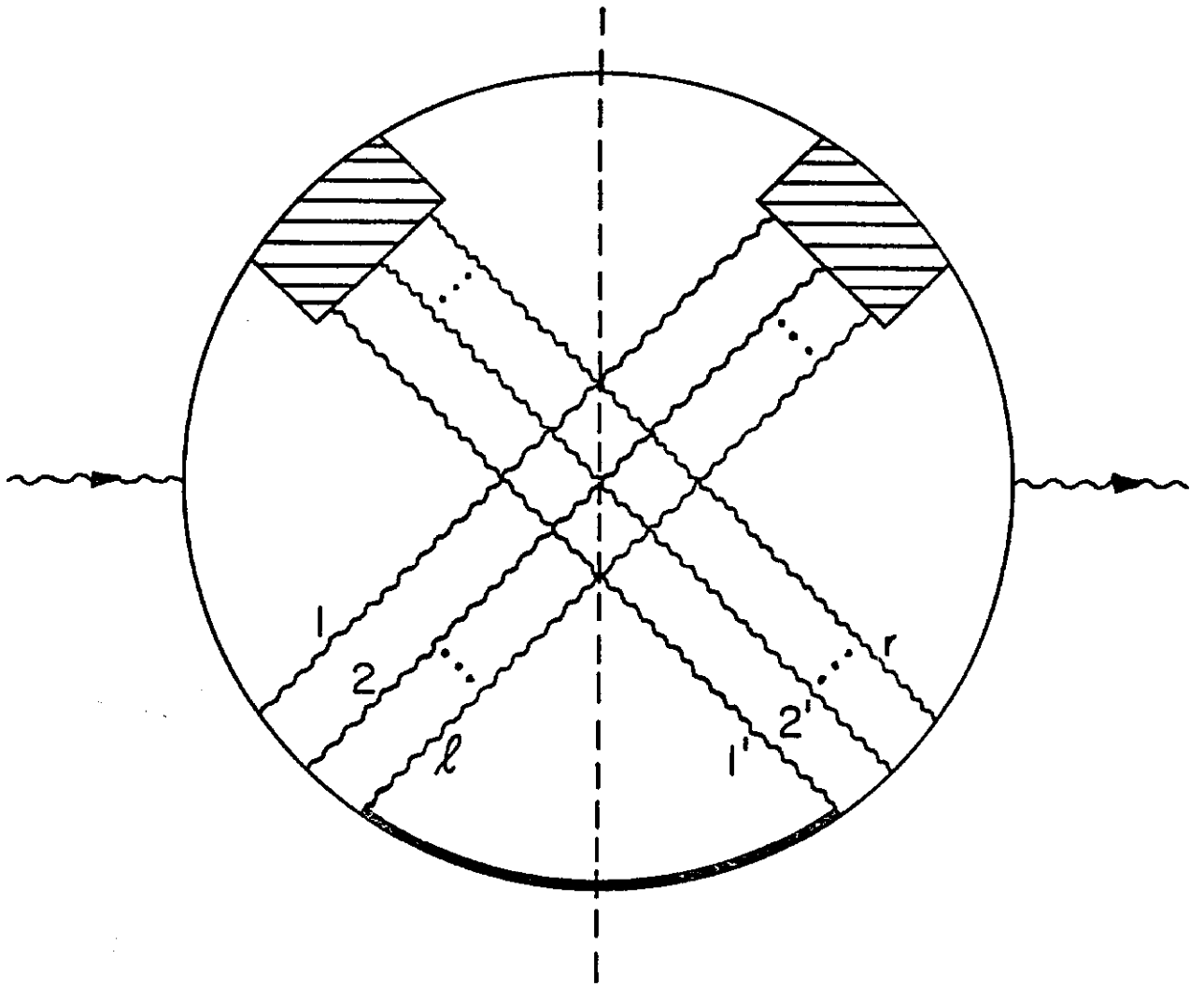


Figure 10

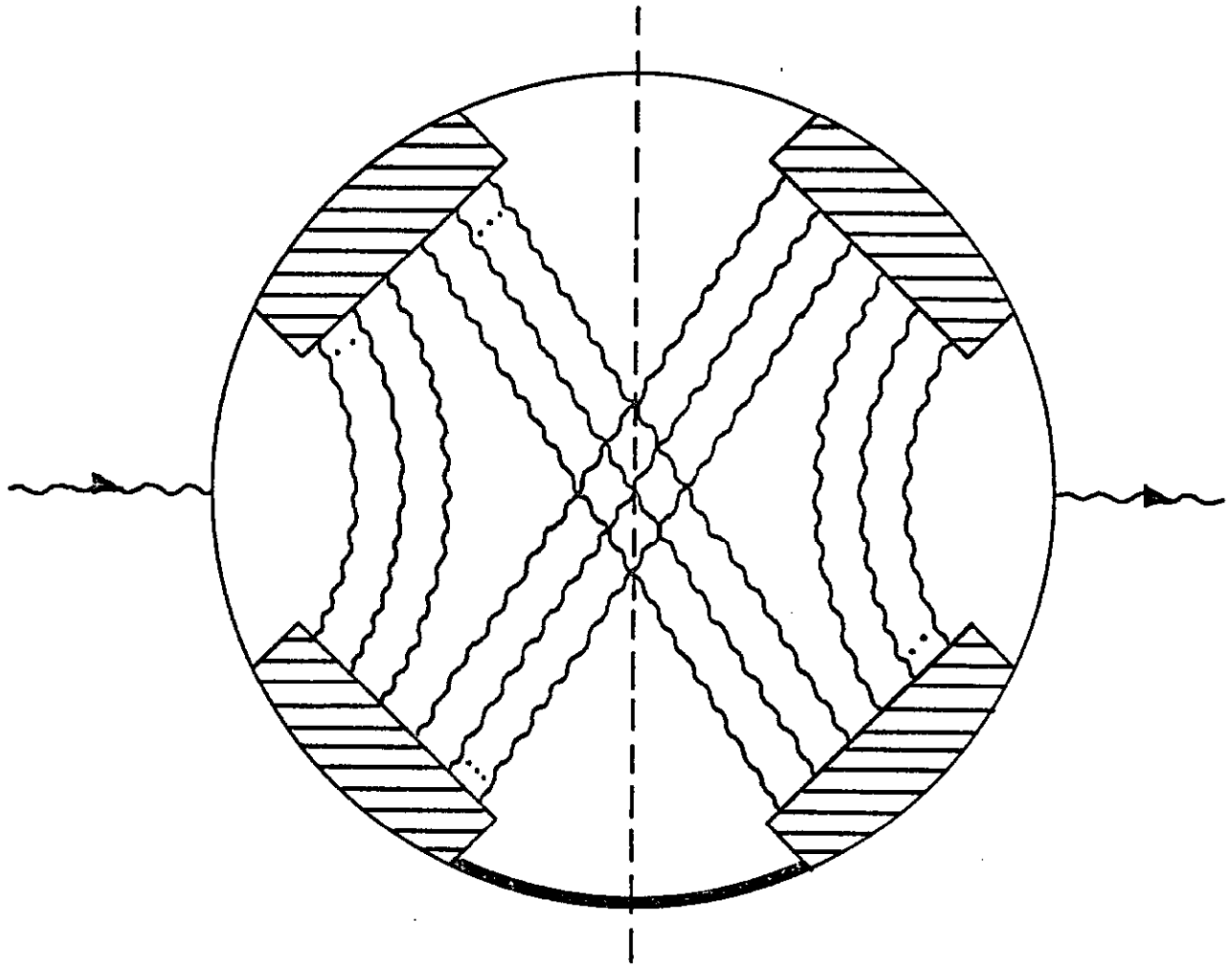


Figure II

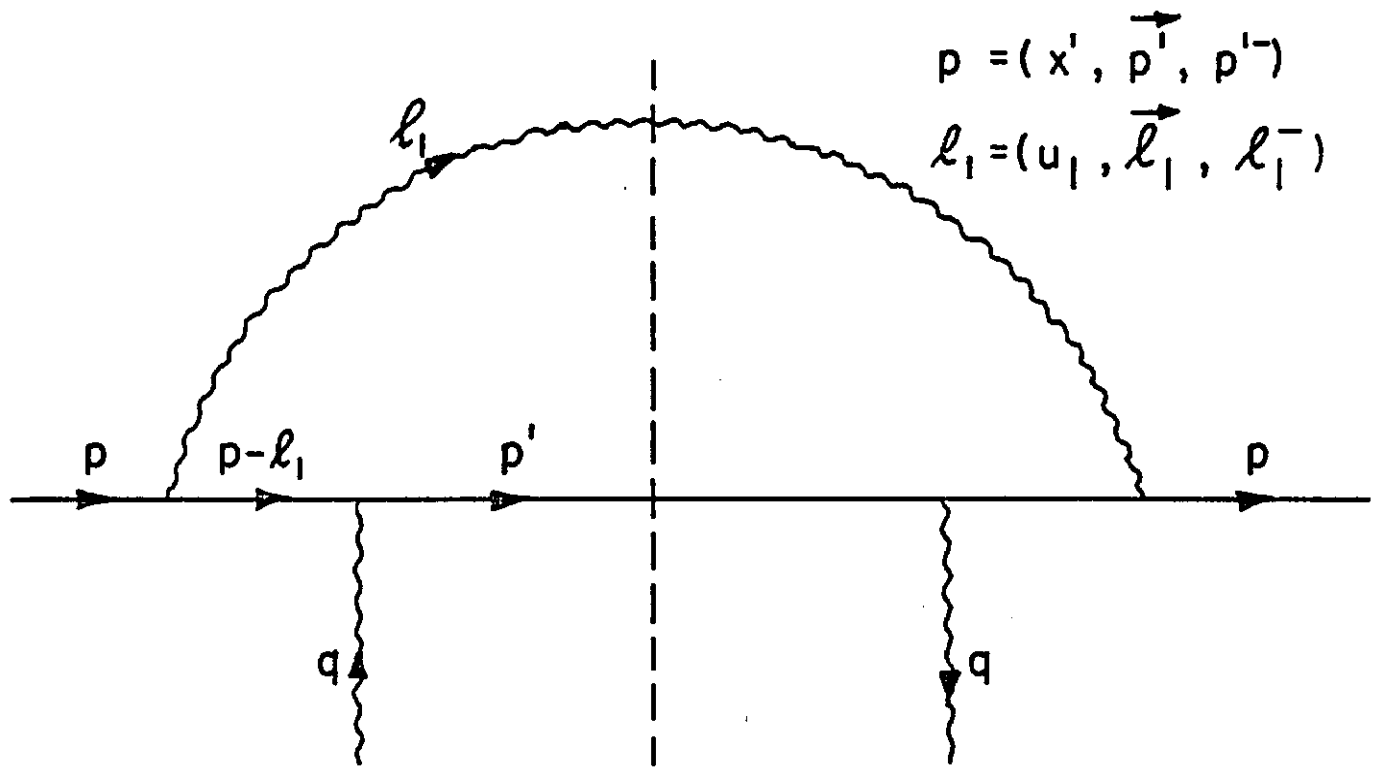
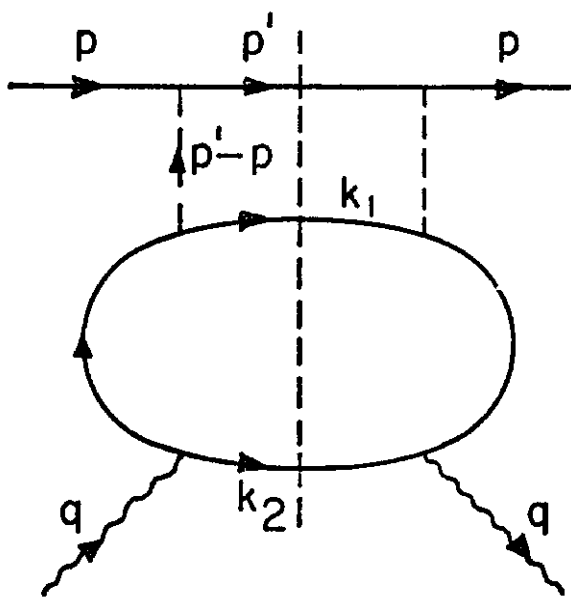
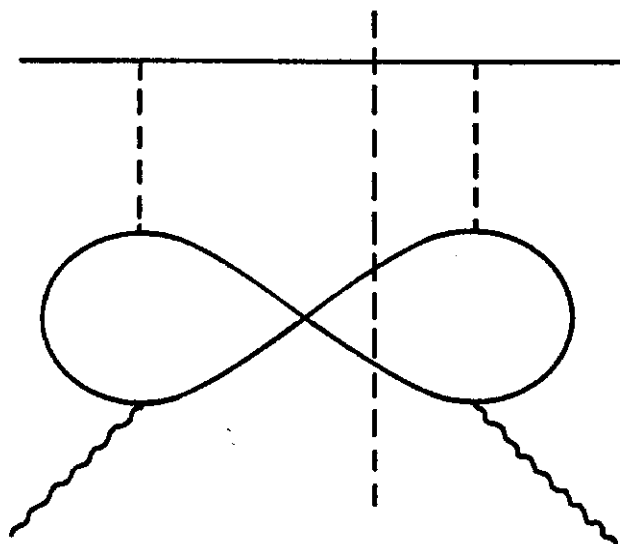


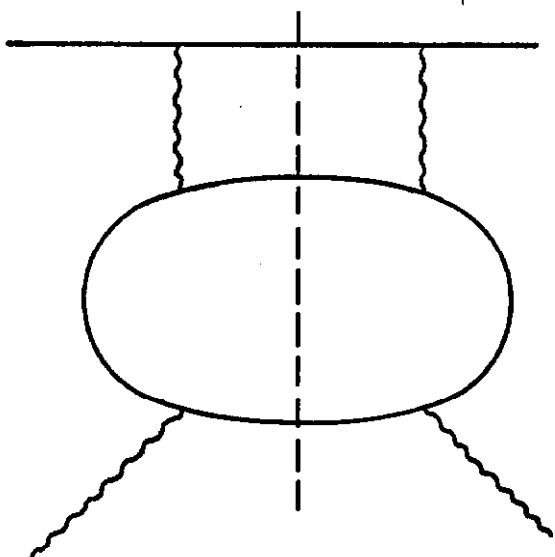
Figure 12



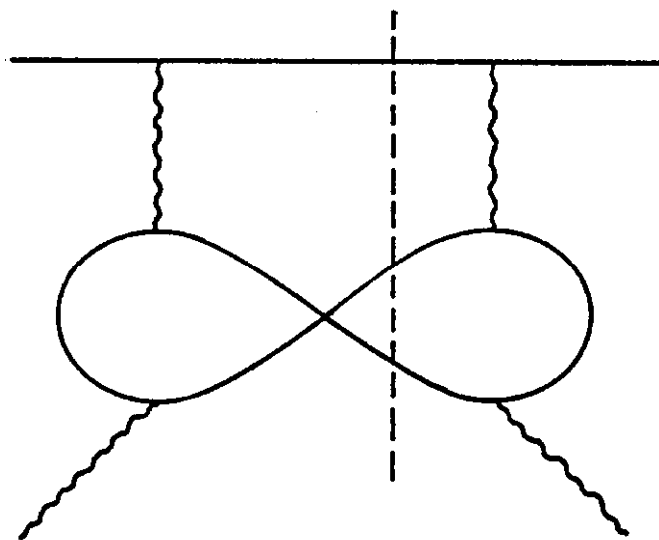
(a)



(b)



(c)



(d)

Figure 13

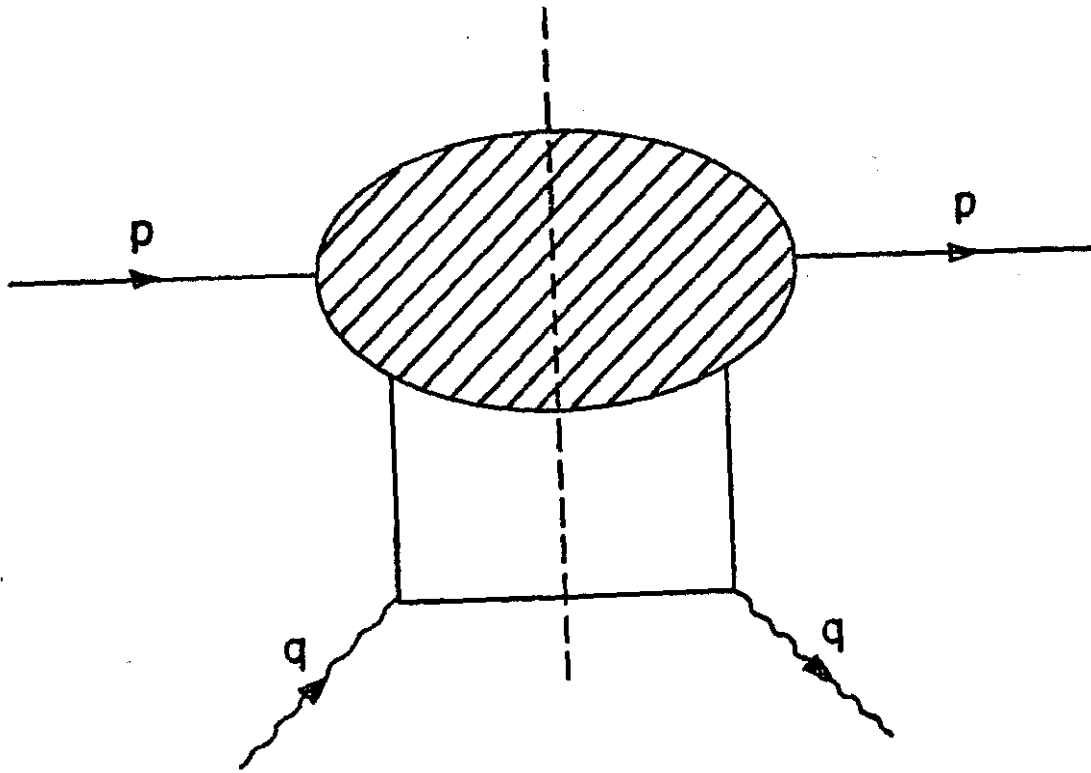


Figure 14

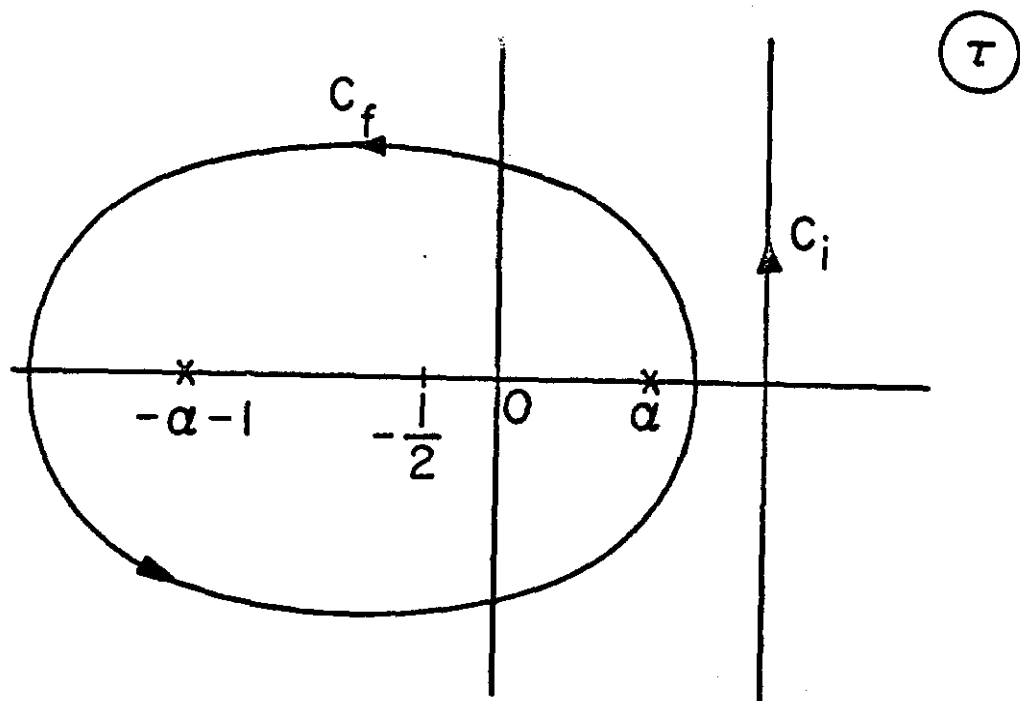


Figure 15

Errata For
 INELASTIC e-p SCATTERING IN MASSIVE
 QUANTUM ELECTRODYNAMICS

P. M. Fishbane and J. D. Sullivan

Phys. Rev. D4, 2516 (1971)

- (i) Fig. 2(c): Interchange k_1 and k_2 labels.
- (ii) Eq. (4.4): Change overall factor from $\left(\frac{m}{8}\right)$ to $\left(\frac{m}{4}\right)$.
- (iii) Change Eq. (A6) to read

$$N = 16 \left\{ (1-x_1) Q^2 + x_1 \vec{Q} \cdot \vec{k}_1 - k_1^2 \right\}.$$

- (iv) Change Eq. (A15) to read

$$(p+q-k_1)^2 \approx x_2 Q^2 (1-x_1-x_2)^{-1}.$$

- (v) In Appendix B when the "seagull" graphs are included the (correct) result becomes $\frac{\nu W_2(\text{scalar})}{\nu W_2(\text{spinor})} = \frac{1+x}{2}$.